

CELL ENGINEERING

A green tea–triggered genetic control system for treating diabetes in mice and monkeys

Jianli Yin¹, Linfeng Yang¹, Lisha Mou², Kaili Dong¹, Jian Jiang¹, Shuai Xue¹, Ying Xu¹, Xinyi Wang¹, Ying Lu², Haifeng Ye^{1*}

Copyright © 2019
The Authors, some
rights reserved;
exclusive licensee
American Association
for the Advancement
of Science. No claim
to original U.S.
Government Works

Cell-based therapies are recognized as the next frontier in medicine, but the translation of many promising technologies into the clinic is currently limited by a lack of remote-control inducers that are safe and can be tightly regulated. Here, we developed therapeutically active engineered cells regulated by a control system that is responsive to protocatechuic acid (PCA), a metabolite found in green tea. We constructed multiple genetic control technologies that could toggle a PCA-responsive ON/OFF switch based on a transcriptional repressor from *Streptomyces coelicolor*. We demonstrated that PCA-controlled switches can be used for guide RNA expression–mediated control of the CRISPR-Cas9 systems for gene editing and epigenetic remodeling. We showed how these technologies could be used as implantable biocomputers in live mice to perform complex logic computations that integrated signals from multiple food metabolites. Last, we used our system to treat type 1 and type 2 diabetes in mice and cynomolgus monkeys. This biocompatible and versatile food phenolic acid–controlled transgenic device opens opportunities for dynamic interventions in gene- and cell-based precision medicine.

INTRODUCTION

Recent advances in cell therapies have required the design of application-specific control systems that are functionalized to perform user-defined, precisely controlled gene editing (1, 2), epigenetic remodeling (3, 4), multilevel biocomputing (5, 6), and specific therapeutic tasks (7–12). Controlling the dynamics of transgene expression is essential for the functionality of these synthetic devices, and such control is particularly relevant in synthetic “designer” cells, engineered cells in which the expression of a transgene determines the dosage of therapeutic outputs produced by the cells when implanted in animals. Engineered cell-based therapies are recognized as the next pillar of medicine, but the advancement of many promising technologies into the clinic is currently limited by the lack of safe and highly specific remote-control triggers to regulate cell behavior after implantation (13, 14).

Initial work in this area used antibiotics such as tetracycline or doxycycline (15) as remote-control triggers for gene expression, but these are not attractive as remote-control switches because, beyond their normal therapeutic function as biocidal molecules, they may lead to the development of antibiotic resistance (16) and side effects (17). Addressing some of these challenges, recently reported remote-control switches can be activated by food or cosmetic preservatives [vanillic acid (VA), benzoate, and phloretin] (18–20). However, these trigger molecules do not occur naturally in foods, have not been demonstrated for long-term use, and could suffer from poor patient compliance (21). It has been proposed that ideal trigger molecules for clinical biomedical applications would be natural, nontoxic, highly soluble, inexpensive, and perhaps even beneficial to health (22). Recently, a caffeine-inducible transgene expression switch was developed for therapeutic output control but is limited by a narrow

dynamic range and relatively low orthogonality (a configuration that avoids signaling cross-talk with endogenous pathways) (23).

Green tea is a globally popular beverage that contains abundant tea polyphenols that are known to reduce the risk of developing cardiovascular diseases and diabetes, among other maladies (24–27). After green tea intake, tea catechins and phenolic acids are rapidly metabolized into the antioxidant protocatechuic acid (PCA) (28). Here, we engineered beverage-triggered, remote-control, transgenic orthogonal switches triggered by PCA from green tea and tested them in mammals. The PCA-controlled switches were designed on the basis of a *Streptomyces coelicolor*–derived transcriptional repressor PcaV (29) fused to eukaryotic epigenetic effector domains that specifically bind to synthetic cognate promoters containing PcaV-specific binding sites. We demonstrated use of our PCAON/OFF switch and related devices in three major bioengineering areas: in CRISPR-Cas9 systems for genome and epigenome engineering, in controllable engineered cell biocomputer implants in live mice, and in controllable engineered cell-based drug delivery systems for treating diabetes in both mouse and monkey models. To further improve the sensitivity of the PCAON switch, we developed a second-generation switch that restored glucose homeostasis in diabetic mice and monkeys after oral administration of PCA or green tea. These beverage-derived phenolic acid–controlled gene circuits expand the synthetic biology toolbox available for constructing safe and clinically relevant cell functions and have the potential to substantially advance gene- and cell-based precision therapies.

RESULTS

Design and validation of PCA-inducible gene switches

To engineer PCA-inducible (PCA_{ON}) gene switches in mammalian cells (Fig. 1A), we constructed a synthetic mammalian transrepressor—PcaR (KRAB-PcaV)—by fusing the human Krueppel-associated box (KRAB) domain to the N terminus of PcaV (Fig. 1B). PcaR binds and silences constitutive gene expression from the synthetic promoter P_{PcaR7} that comprises the human cytomegalovirus promoter (P_{hCMV}) linked (3') to a tandem O_{PcaV} binding site. When PCA is present, it disrupts the PcaR-dependent repression of P_{PcaR7} (Fig. 1B). Assessment

¹Synthetic Biology and Biomedical Engineering Laboratory, Biomedical Synthetic Biology Research Center, Shanghai Key Laboratory of Regulatory Biology, Institute of Biomedical Sciences and School of Life Sciences, East China Normal University, Dongchuan Road 500, Shanghai 200241, China. ²Shenzhen Xenotransplantation Medical Engineering Research and Development Center, Institute of Translational Medicine, Shenzhen Second People's Hospital, First Affiliated Hospital of Shenzhen University, Shenzhen, Guangdong 518035, China.

*Corresponding author. Email: hfy@bio.ecnu.edu.cn

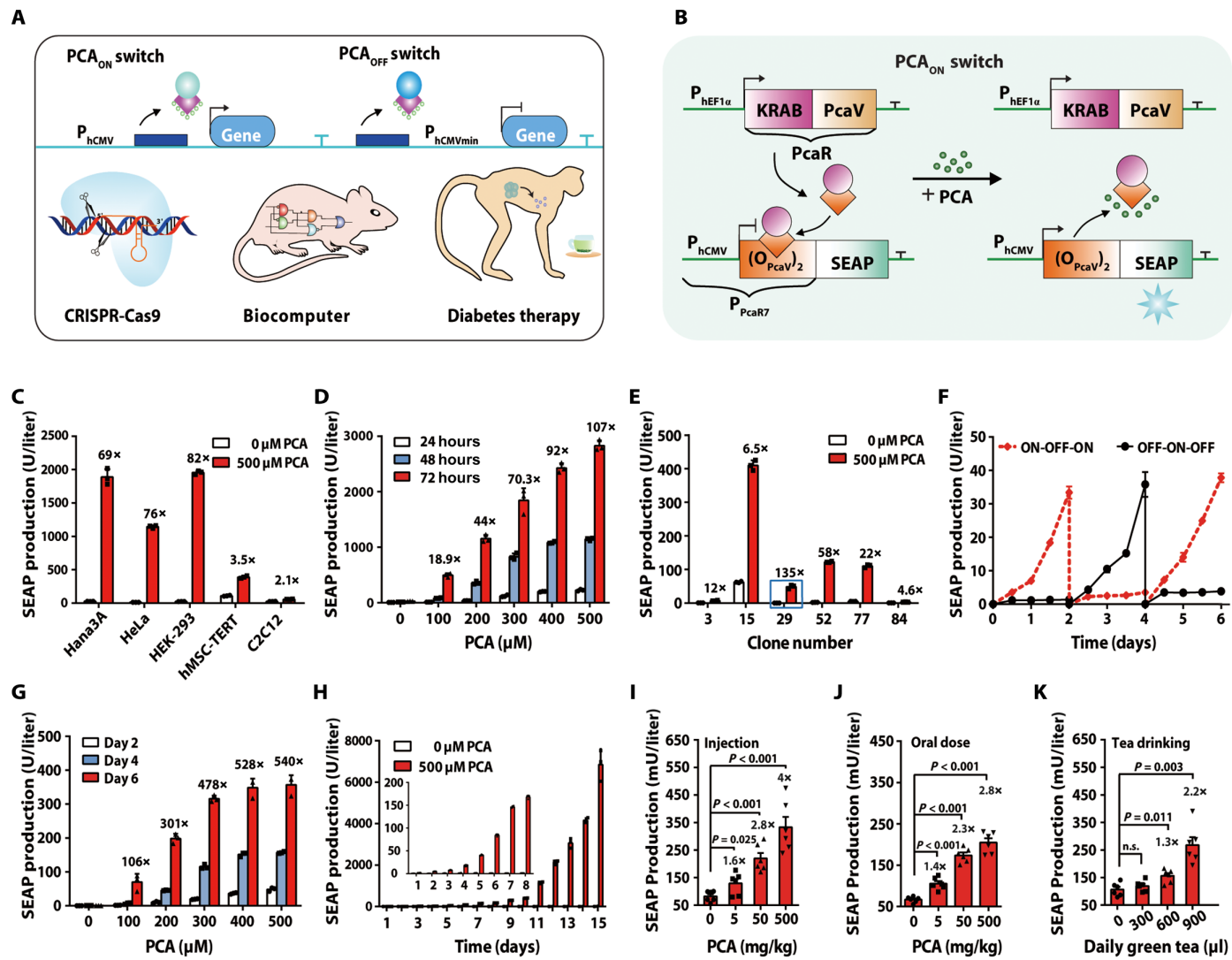


Fig. 1. Design and validation of a PCA-inducible switch (PCA_{ON}) in mammalian cells and mice. (A) Summary of the core design and multiple use cases for the PCA_{ON} gene switch. (B) Detailed schematic for the PCA_{ON} switch design. The synthetic mammalian PCA-triggered transrepressor PcaR (KRAB-PcaV) is an N-terminal fusion of PcaV with a trans-silencing Krueppel-associated box (KRAB) domain: In the absence of PCA, PcaR binds to a chimeric target promoter P_{PcaR7} and represses SEAP expression; in the presence of PCA, PcaR is released from P_{PcaR7} and initiates SEAP expression. (C) PCA-inducible SEAP expression in different mammalian cell lines cotransfected with pJY14 (P_{PcaR7} -SEAP-pA) and pJY29 ($P_{hEF1\alpha}$ -PcaR-pA) was cultivated for 48 hours in the presence or absence of PCA. (D) Dose-dependent PCA-inducible SEAP expression. pJY14/pJY29-transgenic HEK-293 cells were cultivated with different concentrations of PCA. Different color bars represent different time periods for profiling SEAP expression. (E) Selection of stable PCA_{ON} transgenic cell lines (HEK_{PCA-ON}-SEAP) was integrated with pJY14, pJY29, and pJY60 (P_{hCMV} -PuroR-pA). The selected cell clones were profiled for their PCA-inducible SEAP regulation performance. (F) Reversibility of HEK_{PCA-ON}-SEAP-mediated SEAP expression. HEK_{PCA-ON}-SEAP cells (5×10^4) were cultivated for 6 days while alternating the PCA concentrations from 0 to 500 μ M, and SEAP expression in the culture supernatants was profiled every 12 hours. Cell density was adjusted to 5×10^4 every 2 days. (G) Dose-dependent SEAP expression in HEK_{PCA-ON}-SEAP cells. (H) Long-term PCA_{ON}-dependent SEAP expression. (I to K) PCA-dependent SEAP expression in mice. Mice implanted with microencapsulated HEK_{PCA-ON}-SEAP cells received intraperitoneal (I) or oral (J) administration of PCA three times per day (0 to 500 mg kg⁻¹ day⁻¹) or drank different volumes of the concentrated green tea (K) (0 to 900 μ l mouse⁻¹ day⁻¹, equivalent to 0 to 6.3 mg mouse⁻¹ day⁻¹ of total tea polyphenols); SEAP expression in bloodstream was profiled at 48 hours after implantation. The data in (C) to (H) represent the mean \pm SD; $n = 3$ independent experiments. The animal data in (I) to (K) represent the mean \pm SEM; two-tailed Student's *t* test, $n = 6$ mice. n.s., not significant. All individual-level data are in data file S2.

of PCA-mediated toxicity on mammalian cells showed that PCA had no negative effect on either cell viability (fig. S1A) or overall gene expression capacity of the transfected cells within the tested concentration range (fig. S1B). To obtain an optimal PCA_{ON} system permitting minimal basal transgene expression in the absence of PCA and maximal induction rates in the presence of PCA, we optimized the PCA-inducible gene switch by testing different constitutive promoters for driving PcaR expression and different variants of

the synthetic PcaR-specific promoters in human embryonic kidney (HEK)-293 cells. We found that a combination of PcaR and P_{PcaR7} (fig. S2) showed the best induction performance. To address ligand specificity of PcaR, we showed that close chemical analogs of PCA, such as 3,5-dihydroxybenzoate (3,5-DHB) and 3-hydroxybenzoate (3-HB), failed to cross-activate the PCA_{ON} system (fig. S3). Moreover, the pJY14/pJY29-encoded PCA-inducible gene switch worked well in five diverse human and rodent cell types (Fig. 1C). The switch's

strong performance in HEK-293 cells—being dose dependent (Fig. 1D) and time course dependent (fig. S4A) and featuring reversible induction kinetics (fig. S4B)—prompted us to use these cells in our subsequent experiments.

We initially explored the potential for using PCA to monitor engineered cell-based long-term therapies *in vivo* by stably integrating the genetic switch into HEK-293 cells (Fig. 1, E to K). We used the best-in-class monoclonal HEK_{PCA-ON-SEAP} cell line [human placental secreted alkaline phosphatase (SEAP)] (Fig. 1E) and found that our HEK_{PCA-ON-SEAP} cell line showed fully reversible and tunable induction kinetics (Fig. 1, F and G), thus offering excellent switching performance characterized by negligible basal expression and by nonsaturating increases in the transgene output over the course of a 15-day trial (Fig. 1H). We then microencapsulated and implanted these HEK_{PCA-ON-SEAP} cells into mice. Regardless of delivery method (intraperitoneal injection, oral intake from water, or oral intake from concentrated green tea), PCA could control the secretion of a reporter protein SEAP in a dose-dependent manner (Fig. 1, I to K). These results demonstrate *in vivo* that PCA can be used as a trigger for the precise control of implanted engineered cells harboring our PCA_{ON} switch.

PCA-induced and gRNA-mediated control of CRISPR-Cas9 activity

Having established the proof of concept for our PCA_{ON} switch, we next applied it as a regulatory module to control gene editing and epigenetic remodeling. Capitalizing on both the strong activation power of our PCA_{ON} switch (Fig. 1D) and the biocompatibility of PCA for *in vivo* applications (Fig. 1, I to K), we engineered three PCA-inducible CRISPR-Cas9 systems for the guide RNA (gRNA)-dependent inhibition (PcaRi), activation (PcaRa), or deletion (PcaRdel) of endogenous genes in human cells (Fig. 2). Note that our design concept for controlling CRISPR activity was based on the use of the U6 promoter to inducibly drive gRNA expression; previous efforts in controlling gene editing have taken the alternative approach of controlling Cas9 expression or split-Cas9 dimerization (30, 31). We speculated that the tight control of gRNA expression provided another strategy and might decrease the extent of leaky nuclease activity relative to other systems. In our design, O_{PcaV} binding sites were sandwiched upstream and downstream of the U6 (constitutive) promoter that drives expression of the gRNA sequence. As with our PCA_{ON} switch, the engineered PcaR protein binds to these U6-adjacent sites, and PCA activates U6-driven gRNA expression by disrupting this PcaR binding (figs. S5 to S7). We conducted extensive optimization experiments with a SEAP reporter to enable the highly precise control of PCA-induced U6-driven expression and to confirm the success of PCA-controlled CRISPR-Cas9 systems for gRNA-dependent inhibition (PcaRi) and activation (PcaRa) (figs. S5 and S6). We first explored epigenetic remodeling-based gene repression (PcaRi) (Fig. 2A) and ultimately found that an optimal combination of a synthetic PCA-inducible promoter (P_{PcaR13}) driving gRNA expression and a promoter driving dCas9-KRAB expression (P_{PcaR12}) (fig. S5D) allowed for optimal dose-dependent repression of both SEAP and endogenous human gene CXCR4 and TP53 expression (Fig. 2, B to D, and fig. S8, A to C). We next applied the PCA_{ON} switch for the PCA-dependent activation of target genes (PcaRa) (Fig. 2E and fig. S6). For this application, we found that the P_{PcaR15} promoter (harboring five O_{PcaV} repeats both upstream and downstream of the U6 promoter) was optimal (fig. S6, A to D). We also used an expression

strategy based on scaffold gRNAs (32) repurposed for PCA-inducible expression of the synergistic activation mediator complex (SAM: MS2-p65-HSF1) (33) and found that this substantially improved PcaRa performance (fig. S6, E and F): PCA activated both transgene expression and endogenous gene activation (human ASCL1, PDX1) in a dose-dependent manner (Fig. 2, F to H, and fig. S8, D to F).

We also repurposed the PCA-controlled CRISPR-Cas9 system for gene editing (PcaRdel) and used frameshift enhanced green fluorescent protein (fsEGFP)-based assays to test PcaRdel for endogenous gene deletion (Fig. 2I and fig. S7). In these assays, GFP is only expressed after Cas9-mediated cleavage of a target sequence, thereby resulting in error-prone nonhomologous end joining and restoration of a coding reading frame. The promoter P_{PcaR14} showed ideal regulation profiles for gRNA-dependent Cas9 activity, as evaluated with an fsEGFP-based assay (Fig. 2J and fig. S7) (34). We found that a single gRNA targeting the human CCR5 and EMX1 genes was sufficient to reveal PCA-induced indel formations (Fig. 2, K and L), demonstrating highly efficient and tight regulation of the targeted deletion of genome sequences in human cells. Thus, as they facilitate the tight induction of CRISPR activities for the dynamic control of endogenous genes (with modes for repression, activation, and deletion), our three new PCA-inducible CRISPR-Cas9 devices are suitable for use in applications requiring the precise control of genome or epigenome editing.

Engineered PCA- and VA-controlled biocomputational cell implants in mice

Information processing in biological systems can be achieved using rationally assembled Boolean logic gates that allow cells to sense the presence of defined input signals and respond with a computer-like algorithm (35, 36). Although human cells have previously been programmed to perform complex logics *in vitro*, the concept of programmable biocomputing in animals has remained elusive due to issues with biocompatibility and the toxicity of antibiotic-based trigger compounds (5, 37). Here, seeking to illustrate a generalizable biocomputation platform controlled by food-derived phenolic acids *in vivo*, we combined our PCA_{ON} system with a previously reported VA-based transgene control system (18). Our design uses five logic gates (figs. S9 and S10) to enable a variety of operations.

First, two VA-controlled transgene expression switches (VA_{ON} and VA_{OFF}) were constructed and validated (fig. S11). The NIMPLY circuits are exclusively induced only in the presence of one of the two inputs. To program the PCA NIMPLY VA logic gate, we engineered a hybrid promoter P_{PV1} [P_{1VanO2}-(O_{PcaV})₂] comprising a VA-repressible promoter (P_{1VanO2}) fused with a PcaR binding site (O_{PcaV})₂, allowing the presence of only PCA to permit output gene expression (figs. S9A and S10A). To engineer the reversed VA NIMPLY PCA logic gate, a PCA_{OFF} switch was developed (fig. S12), and a PCA-repressible promoter (P_{PcaA1}) fused with a VanR binding box (VanO₄) was formed into a hybrid promoter P_{PV2} (P_{PcaA1}-VanO₄) controlled by the synthetic transactivator PcaA (PcaV-VP16), which permits signal output only in the presence of VA (figs. S9B and S10B).

An AND gate is a digital logic gate with two or more inputs and one output that performs logical conjunction. To create an AND gate, we engineered a synthetic promoter (P_{PV3}) based on P_{hCMV} symmetrically flanked by tandem O_{PcaV} and O_{VanR} binding sites, meaning that output gene expression was only permitted when both VA and PCA were present to derepress constitutive promoter activity (figs. S9C and S10C). To create an OR gate, which is a logical gate

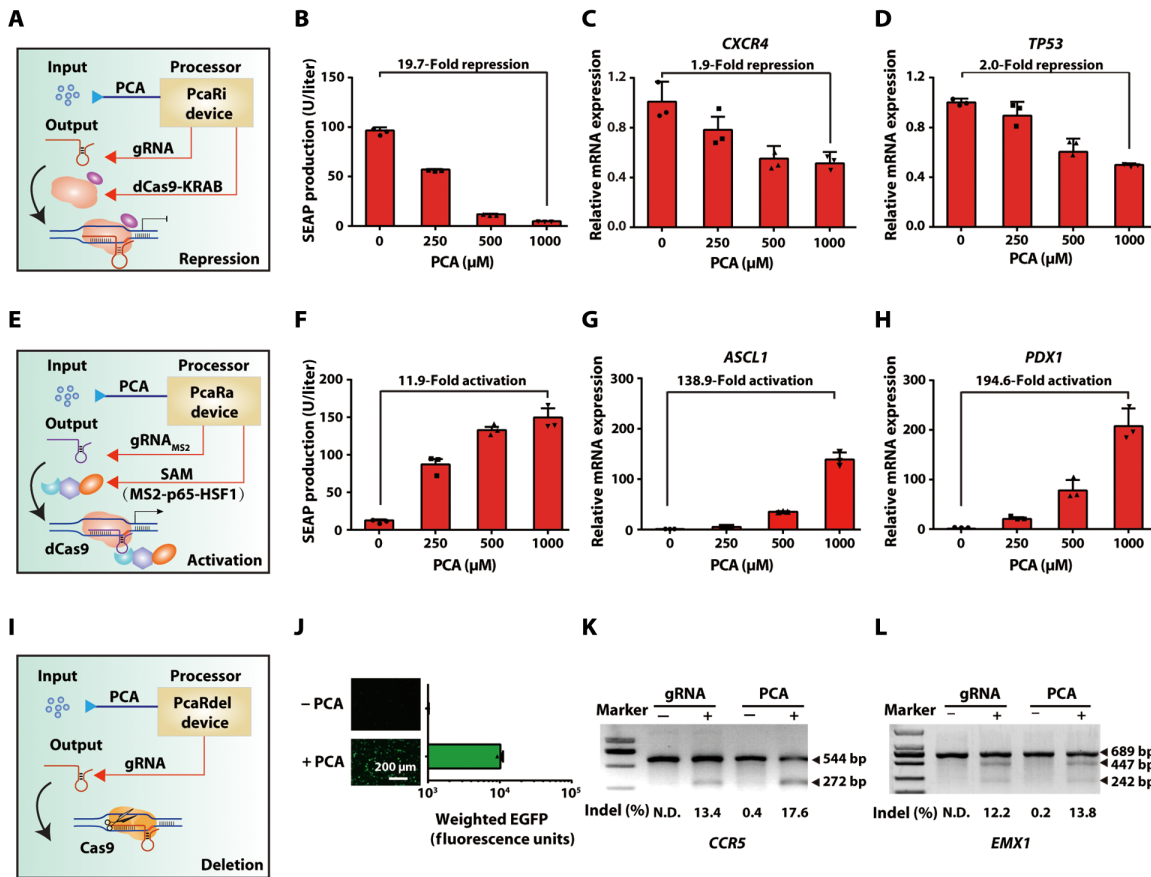


Fig. 2. PCA-controlled CRISPR-Cas9 devices for genome and epigenome editing. (A) Schematic design of PCA-controlled PcaR-mediated inhibition (PcaRi). In the presence of PCA, the expression of both gRNA and dCas9-KRAB is induced to assemble into a repressive complex (gRNA-dCas9-KRAB) that targets a specific DNA site to inhibit gene expression. (B) Dose-dependent PCA-repressible SEAP expression for PcaRi. HEK-293 cells were cotransfected with pJY19 ($P_{\text{CAG}}\text{-PcaR-pA}$), pJY131 ($P_{\text{PcaR13}}\text{-dCas9-KRAB-pA}$), pJY109 ($P_{\text{gRNA13-SEAP-pA}}$), and pJY53 ($P_{\text{PcaR13-gRNA}_{\text{ASCL1}}}$) and cultivated with various PCA concentrations. SEAP expression was profiled after 48 hours. (C and D) PcaRi-mediated inhibition of endogenous gene expression. HEK-293 cells were cotransfected with pJY19, pJY131, pWL67 ($P_{\text{PcaR13-gRNA}_{\text{CXCR4}}}$) (C), or pWL66 ($P_{\text{PcaR13-gRNA}_{\text{TP53}}}$) (D) and cultivated for 48 hours with various PCA concentrations. The relative mRNA expression of CXCR4 (C) and TP53 (D) was quantified by qPCR. (E) Schematic design of PCA-controlled PcaR-mediated activation (PcaRa). In the presence of PCA, gRNA_{MS2} (gRNA with MS2 loop) and the transactivator MS2-p65-HSF1 are produced to recruit constitutively expressed dCas9 to form a transcriptional activation complex (gRNA_{MS2}-dCas9-MS2-p65-HSF1). (F) Dose-dependent PCA-inducible SEAP expression for PcaRa. HEK-293 cells were cotransfected with pJY19, pSZ69 ($P_{\text{hCMV}}\text{-dCas9-pA}$), pJY137 ($P_{\text{PcaR2-MS2-p65-HSF1-P2A-EGFP-pA}}$), pJY110 ($P_{\text{gRNA2-SEAP-pA}}$), and pJY57 ($P_{\text{PcaR14-gRNA}_{\text{ASCL1(MS2)}}}$) and cultivated with various PCA concentrations. SEAP expression was profiled after 48 hours. (G and H) PcaRa-mediated activation of endogenous gene expression. HEK-293 cells were cotransfected with pJY19, pSZ69, pJY137, and pJY57 (G) or pJY55 ($P_{\text{PcaR14-gRNA}_{\text{PDX1(MS2)}}}$) (H) and cultivated for 48 hours with various PCA concentrations. The relative mRNA expression of ASCL1 (G) and PDX1 (H) was quantified by qPCR. (I) Schematic design of PCA-controlled PcaR-mediated gene deletion (PcaRdel). gRNA expression is induced by PCA and enables Cas9-mediated target gene deletion. (J) Correction of frameshift EGFP (fsEGFP) expression with PcaRdel. HEK-293 cells were cotransfected with pJY19 ($P_{\text{CAG}}\text{-PcaR-pA}$), pJY58 ($P_{\text{PcaR14-gRNA}_{\text{CCR5}}}$), pYW54 ($P_{\text{hCMV}}\text{-Cas9-pA}$), and pJY221 ($P_{\text{hCMV}}\text{-fsEGFP-pA}$) and cultivated in the presence or absence of 500 μM PCA. EGFP expression was profiled by fluorescence microscopy and flow cytometric analysis after 24 hours. The data (B to D, F to H, and J) represent the mean \pm SD; $n = 3$ independent experiments. (K and L) PcaRdel-mediated genome editing. HEK-293 cells were cotransfected with pJY19 and pYW54, as well as pJY58 (K) or pJY59 ($P_{\text{PcaR14-gRNA}_{\text{EMX1}}}$) (L) and cultivated for 48 hours in the presence or absence of 500 μM PCA. Control cells were cotransfected with a constitutive Cas9 expression vector, as well as mismatched or matched gRNAs as negative or positive controls, respectively. Indel mutation frequencies of the CCR5 (K) and EMX1 (L) loci were evaluated using mismatch-sensitive T7E1 assays ($n = 1$ from two independent experiments). Black arrows indicate the expected cleavage bands. N.D., not detectable. All individual-level data are in data file S2.

that produces inclusive disjunction, we used parallel PCA_{ON} and VA_{ON} switches controlling the expression of a single-shared transactivator (GV: Gal4-VP16). Either or both inputs permitted the expression of the transactivator GV that constitutively activates output gene expression from a Gal4-specific minimal promoter (P_{UAS}) (figs. S9D and S10D). A NOR gate is “ON” only when both inputs are absent. Last, PCA_{OFF} and VA_{OFF} switches each control the expression of a split transactivator (TetR-DocS::Coh2-VP16) that enabled the creation of a NOR gate, for which only the simultaneous absence of

VA and PCA permits the expression and formation of a full complete transactivator that permits the minimal promoter ($P_{\text{hCMV}^{*-1}}$) to drive output gene expression (figs. S9E and S10E).

After successfully demonstrating the PCA- and VA-controlled programmable logic gate biocomputers in mammalian cells, we next tested their functionality in mice (Fig. 3). Aiming to simulate the controlled release of therapeutic proteins *in vivo*, we replaced the fluorescent reporter protein d2EYFP with the secretory protein SEAP and implanted microencapsulated cells programmed to perform

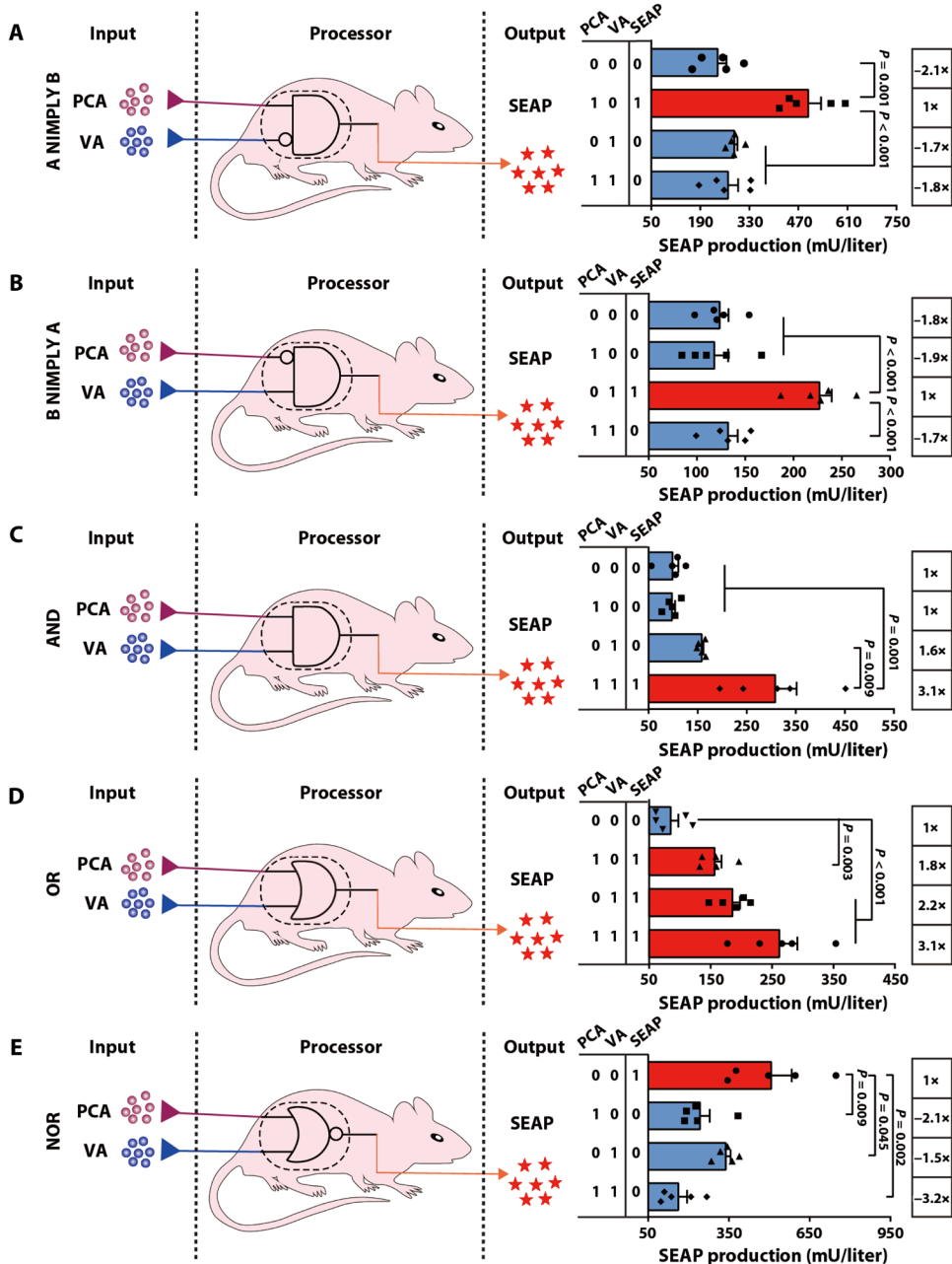


Fig. 3. PCA- and VA-controlled programmable biocomputers in mice. The processing performance of the (A) A NIMPLY B, (B) B NIMPLY A, (C) AND, (D) OR, and (E) NOR logic gates in the implanted biocomputer in mice. Mice were intraperitoneally implanted with 2×10^6 microencapsulated (A) pJY29-/pJY162-/pJY179, (B) pJY12-/pJY159-/pCK189, (C) pJY29-/pCK189-/pJY303, (D) pJY29-/pDL24-/pCK189-/pDL30-/pDL6, and (E) pJY12-/pJY201-/pJY179-/pJY200-/pMF111 transgenic HEK-293 cells; these mice received thrice daily injections of different combinations of the two input signals PCA ($500 \text{ mg kg}^{-1} \text{ day}^{-1}$) and VA ($500 \text{ mg kg}^{-1} \text{ day}^{-1}$) in accordance with the truth table. The SEAP expression in the bloodstream was profiled at 48 hours after implantation. All data represent the mean \pm SEM; two-tailed Student's *t* test, $n = 5$ mice. See table S3 for detailed description of genetic components and table S6 for detailed transfection mixtures for each logic gate. All individual-level data are in data file S2.

NIMPLY (Fig. 3, A and B), AND (Fig. 3C), OR (Fig. 3D), or NOR (Fig. 3E) logic operations into mice. We administered PCA and VA to mice in various combinations, and quantification of SEAP in the bloodstream of the mice validated the logic operations of all gate types (Fig. 3). As expected, SEAP expression in both NIMPLY circuits

significantly ($P = 0.001$ or $P < 0.001$) increased only in the presence of the input specific to that circuit (PCA or VA) (Fig. 3, A and B). Moreover, quantitative SEAP profiling of the AND gate showed high output signal in the presence of both PCA and VA (Fig. 3C). The OR gate revealed low SEAP leakage when in the absence of both PCA and VA and increased SEAP expression in the presence of either or both inputs (Fig. 3D). Contrary to the OR gate, the NOR gate in mice revealed high SEAP production when in the absence of both PCA and VA and low output signal when in the presence of either or both inputs (Fig. 3E). These exciting proof-of-principle results for whole-animal bio-computing demonstrate that complex living genetic programs (therapeutic implants) can be remotely controlled using food phenolic acids. Practically, the devices that we developed in our proof-of-principle experiments represent modular components that can be used in future precision engineering of increasingly complex engineered cell-based therapeutic dosing regimens in animals.

PCA-regulated engineered cells for diabetes therapy in mice

After validating PCA administration-triggered controlled drug delivery over a series of weeks in mice (Fig. 4A), we tested the potential of the PCA_{ON} system for treating experimental diabetes. On the basis of PCA_{ON} switch 1.0, we engineered two different stable cells: one allowing for PCA-inducible expression of SEAP and insulin (fig. S13A) and the other producing a short variant of human glucagon-like peptide 1 (shGLP-1) and SEAP (fig. S13B) (38, 39). When these stable cells were implanted into mouse models of type 1 (Fig. 4, B to D) and type 2 diabetes mellitus (Fig. 4, E to I), respectively, significantly induced insulin (Fig. 4B) and shGLP-1 (Fig. 4E) restored homeostatic fasting blood glucose concentrations (Fig. 4, C and F) and glucose tolerance (Fig. 4, D and G) upon PCA injection. Although the antidiabetic activities were observed in both mice (Fig. 4, B to I), compared with injection of PCA, an orally administered PCA or green tea drinking program

is more attractive with respect to patient compliance. However, the 1.0 version of the PCA_{ON} system was not sufficiently robust to produce therapeutic efficiency through oral PCA administration (Fig. 1).

Seeking to decrease the amount of PCA needed to trigger our induction system and ultimately aiming to enable oral treatment

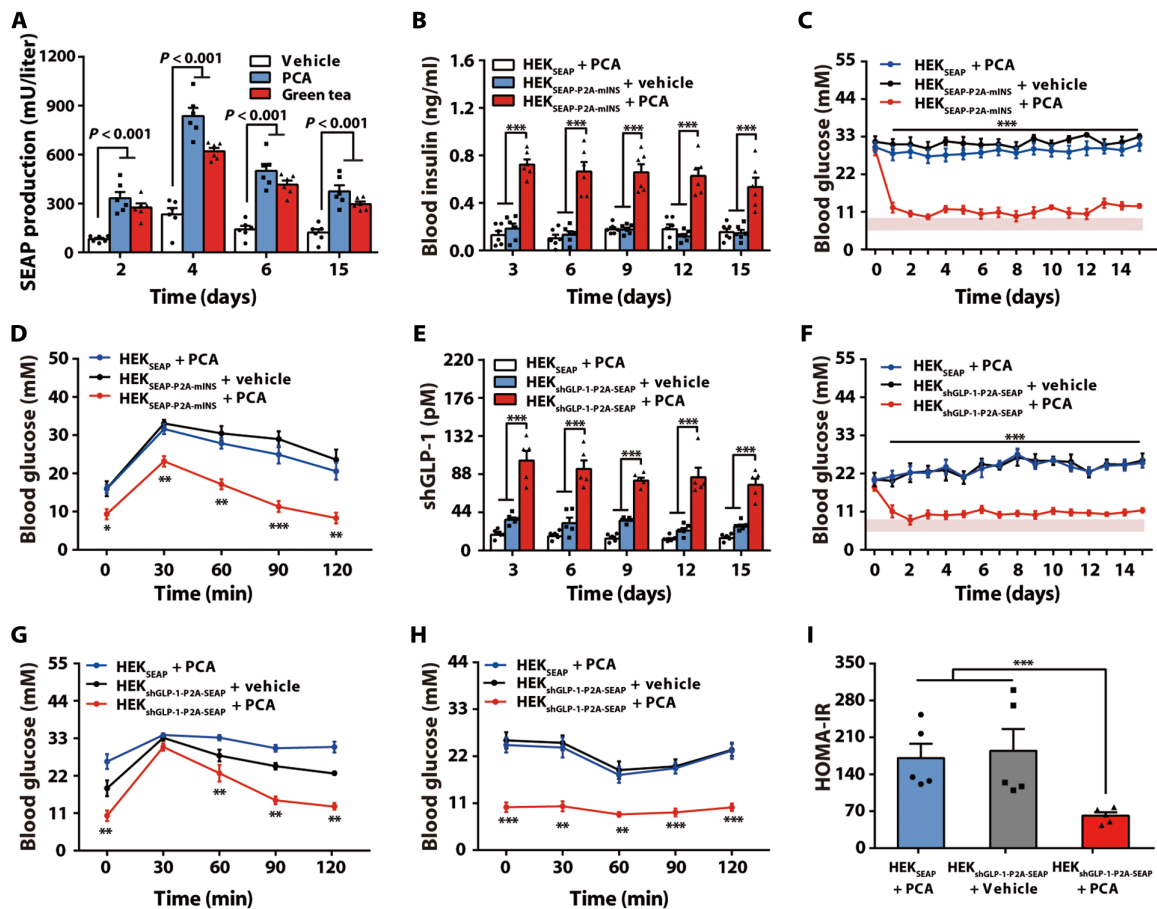


Fig. 4. PCA_{ON}-1.0 switch-controlled treatment of type 1 and type 2 diabetic mice. (A) Long-term PCA_{ON}-regulated SEAP expression in mice. Mice implanted with 2×10^6 microencapsulated HEK_{PCA-ON-SEAP} cells (200 cells per capsule) received thrice daily injections of PCA ($500 \text{ mg kg}^{-1} \text{ day}^{-1}$) or oral administration of concentrated green tea ($900 \mu\text{l mouse}^{-1} \text{ day}^{-1}$). SEAP expression in the bloodstream of mice was monitored for 15 days. (B to D) PCA-dependent treatment of type 1 diabetic mice. Type 1 diabetic mice were intraperitoneally implanted with 3×10^6 microencapsulated HEK_{PCA-ON-SEAP-P2A-mINS} cells and received thrice daily PCA injections ($500 \text{ mg kg}^{-1} \text{ day}^{-1}$). Control mice were implanted with negative-control implants (HEK_{PCA-ON-SEAP} cells) and received PCA injections, or mice received therapeutic implants (HEK_{PCA-ON-SEAP-P2A-mINS} cells) but without PCA administration. (B) Blood insulin and (C) blood glucose were profiled for up to 15 days after implantation. (D) Intraperitoneal glucose tolerance test (IPGTT) was conducted on day 5 after implantation. (E to I) PCA-dependent treatment of type 2 diabetic mice. Type 2 diabetic mice were intraperitoneally implanted with 3×10^6 microencapsulated HEK_{PCA-ON-shGLP-1-P2A-SEAP} cells and received thrice daily PCA injections ($500 \text{ mg kg}^{-1} \text{ day}^{-1}$). Control mice were implanted with negative-control implants (HEK_{PCA-ON-SEAP} cells) and received PCA injections, or mice received therapeutic implants (HEK_{PCA-ON-shGLP-1-P2A-SEAP} cells) but without PCA administration. Blood (E) shGLP-1 and (F) glucose were quantified for up to 15 days after implantation. (G) IPGTT and (H) insulin tolerance test (ITT) were conducted, respectively, on days 5 and 7 after implantation. (I) Homeostasis model assessment of insulin resistance (HOMA-IR) was analyzed on day 12 after implantation. Pink area represents normal blood glucose range. All data represent the mean \pm SEM; two-tailed Student's *t* test, *n* = 5 or 6 mice. **P* < 0.05, ***P* < 0.01, ****P* < 0.001 versus control. All individual-level data are in data file S2.

based on oral administration of PCA or green tea, we were motivated to substantially improve the sensitivity of our PCA_{ON} switch. PCA_{ON} switch version 2.0 proved to be much more sensitive to PCA than our initial switch and increased intracellular concentrations of PCA. We used a known PCA transporter protein (PcaK) from *Acinetobacter* sp., ADP1 (40), to pump PCA into our engineered cells (Fig. 5A). The pJY14/pJY29/pJY322 (P_{hCMV}-PcaK-Pa)–encoded PCA-inducible gene switch version 2.0 showed much better transgene expression performance than the initial version (PCA_{ON}-switch 1.0) in HEK-293 cells, with dose- and time course–dependent induction kinetics, especially at lower PCA concentrations (5 to 80 μM) (Fig. 5, B and C). On the basis of the PCA_{ON} switch 2.0, we next constructed and selected two high-sensitive and inducible isogenic cell clones that allowed for PCA-inducible transgene expression of insulin and SEAP (HEK_{PCA-ON-2.0-SEAP-P2A-mINS}) or shGLP-1 and SEAP (HEK_{PCA-ON-2.0-shGLP-P2A-SEAP}). The PCA_{ON}

switch 2.0 showed much greater transgene induction than the PCA_{ON} switch 1.0 by more than 700-fold, partly due to the very low background expression (Fig. 5, D and E). When the microencapsulated HEK_{PCA-ON-2.0-shGLP-P2A-SEAP} cells were implanted into mice, regardless of delivery method (intraperitoneal injection, oral intake of PCA, or concentrated green tea), PCA could control transgene expression in a dose-dependent manner (Fig. 5, F to H). These results demonstrate that the PCA_{ON} switch 2.0 is more sensitive to PCA with better transgene induction fold both in mammalian cells and in mice.

To demonstrate the antidiabetic efficacy, type 1 (Fig. 6, A to C) and type 2 (Fig. 6, D to H) diabetic mice were intraperitoneally implanted with microencapsulated HEK_{PCA-ON-2.0-SEAP-P2A-mINS} and HEK_{PCA-ON-2.0-shGLP-P2A-SEAP} cells, respectively. In both disease models, induced insulin (Fig. 6A) or shGLP-1 (Fig. 6D) expression was sufficient to restore homeostatic fasting glycemia (Fig. 6, B and E)

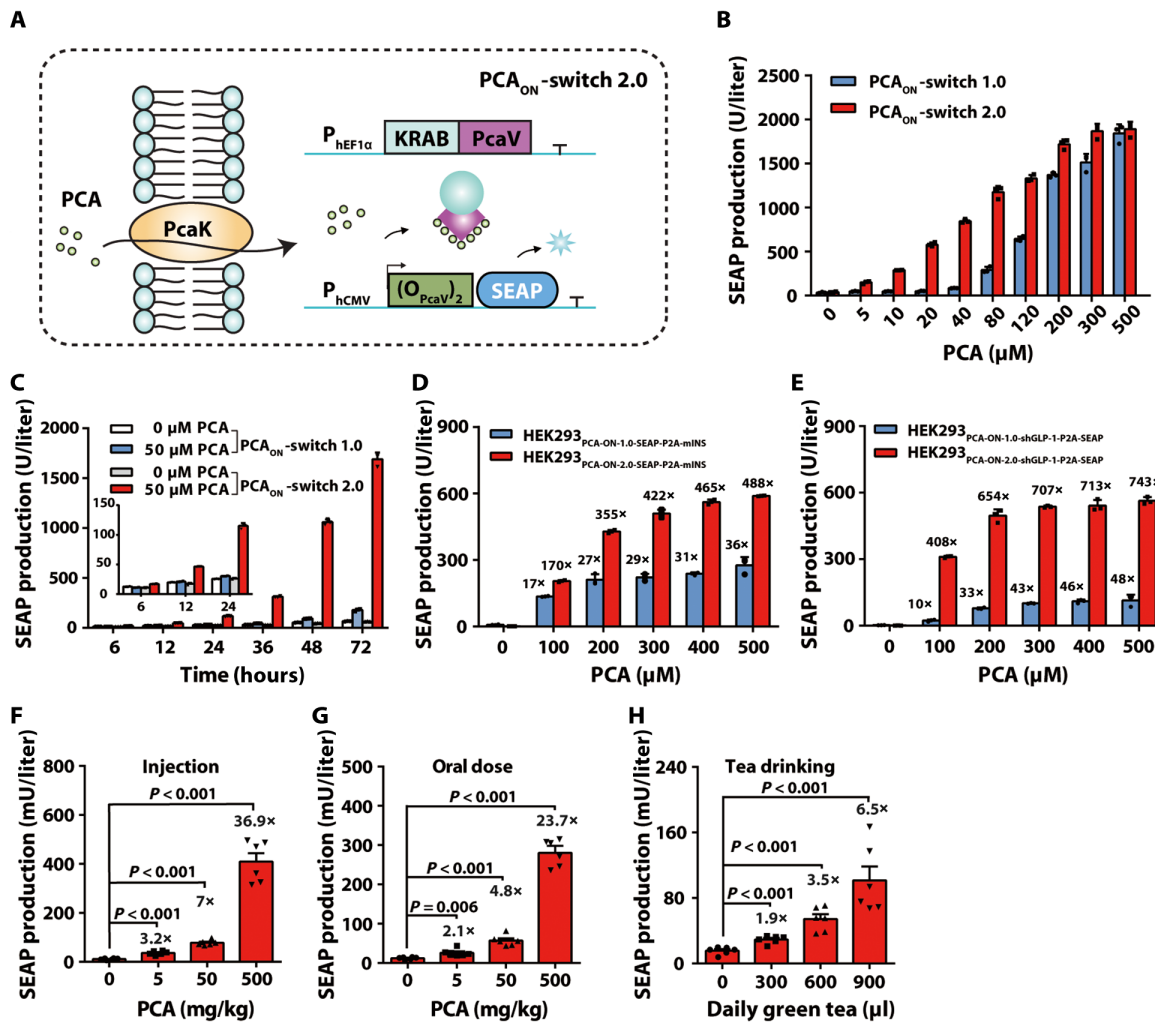


Fig. 5. Design and validation of the PCA_{ON} switch 2.0 version (PCA_{ON}-2.0) in mammalian cells and mice. (A) Detailed schematic for the PCA_{ON}-2.0 switch design. On the basis of the PCA_{ON}-1.0 switch, the enhanced version PCA_{ON}-2.0 was designed based on pumping more PCA into engineered cells by a PCA transporter. In the presence of the transporter PcaK, PCA molecules were easily pumped from culture medium into cells, which results in the release of PcaR from P_{PcaR7} and the initiation of SEAP expression in a relative low PCA concentration. **(B)** Dose-dependent SEAP expression kinetics of the PCA_{ON}-2.0 switch compared with PCA_{ON}-1.0 switch. HEK-293 cells were transfected with either PCA_{ON}-1.0 switch (pJY29/pJY14) or PCA_{ON}-2.0 switch (pJY29/pJY14/pJY322) and cultivated with different concentrations of PCA. SEAP expression was profiled after 48 hours. **(C)** Time-dependent SEAP expression kinetics of the PCA_{ON}-2.0 switch compared with PCA_{ON}-1.0 switch. HEK-293 cells were transfected with either PCA_{ON}-1.0 switch (pJY29/pJY14) or PCA_{ON}-2.0 switch (pJY29/pJY14/pJY322) and cultivated for 72 hours in the presence or absence of 50 μM PCA. **(D)** HEK-293 cells transgenic for PCA_{ON}-1.0- or PCA_{ON}-2.0-inducible SEAP and mouse insulin expression (HEK_{PCA-1.0-SEAP-P2A-mINS} or HEK_{PCA-2.0-SEAP-P2A-mINS}) were cultivated in medium containing various PCA concentrations. SEAP expression in the culture supernatants was profiled after 48 hours. **(E)** HEK-293 cells transgenic for PCA_{ON}-1.0- or PCA_{ON}-2.0-inducible SEAP and shGLP-1 expression (HEK_{PCA-1.0-shGLP-1-P2A-SEAP} or HEK_{PCA-2.0-shGLP-1-P2A-SEAP}) were cultivated in medium-containing various PCA concentrations. SEAP expression in the culture supernatants was profiled after 48 hours. **(F to H)** PCA_{ON}-2.0-dependent SEAP expression in wild-type mice. Mice implanted with microencapsulated HEK_{PCA-ON-2.0-shGLP-1-P2A-SEAP} cells received intraperitoneal (F) or oral (G) administration of PCA three times per day (0 to 500 $\text{mg kg}^{-1} \text{ day}^{-1}$) or drank different volumes of the concentrated green tea (H) (0 to 900 $\mu\text{l} \text{ mouse}^{-1} \text{ day}^{-1}$); SEAP expression in bloodstream was profiled at 48 hours after implantation. The data in (B) to (E) represent the mean \pm SD; $n = 3$ independent experiments. The animal data in (F) to (H) represent the mean \pm SEM; two-tailed Student's *t* test, $n = 6$ mice. All individual-level data are in data file S2.

and glucose tolerance (Fig. 6, C and F) upon either oral administration of PCA (500 $\text{mg kg}^{-1} \text{ day}^{-1}$) or the concentrated green tea (900 $\mu\text{l} \text{ mouse}^{-1} \text{ day}^{-1}$). Moreover, PCA treatment of the implanted type 2 diabetic mice resulted in substantially improved insulin tolerance (Fig. 6G) and insulin sensitivity (Fig. 6H) within 2 weeks. In the type 1 diabetic mouse model, dose-dependent insulin expression was inducible by oral administration of PCA (fig. S14A), with maximal hypoglycemic effects including homeostatic fasting glycemia and glucose tolerance being most pronounced in the highest dosage group (500 $\text{mg kg}^{-1} \text{ day}^{-1}$) (fig. S14, B and C); even the lowest tested oral PCA dose (100 mg kg^{-1}

day^{-1}) led to sufficient improvements in insulin expression to control blood glucose homeostasis (fig. S14). Control experiments showed that oral administration of PCA or tea drinking alone did not induce hypoglycemic effect in the diabetic mice (fig. S15).

PCA-regulated engineered cells for diabetes therapy in nonhuman primates

It is widely accepted that rodent models often do not reflect human conditions faithfully; this issue has limited the translation of engineered cell-based diabetes therapies into first-in-human clinical trials (36, 37).

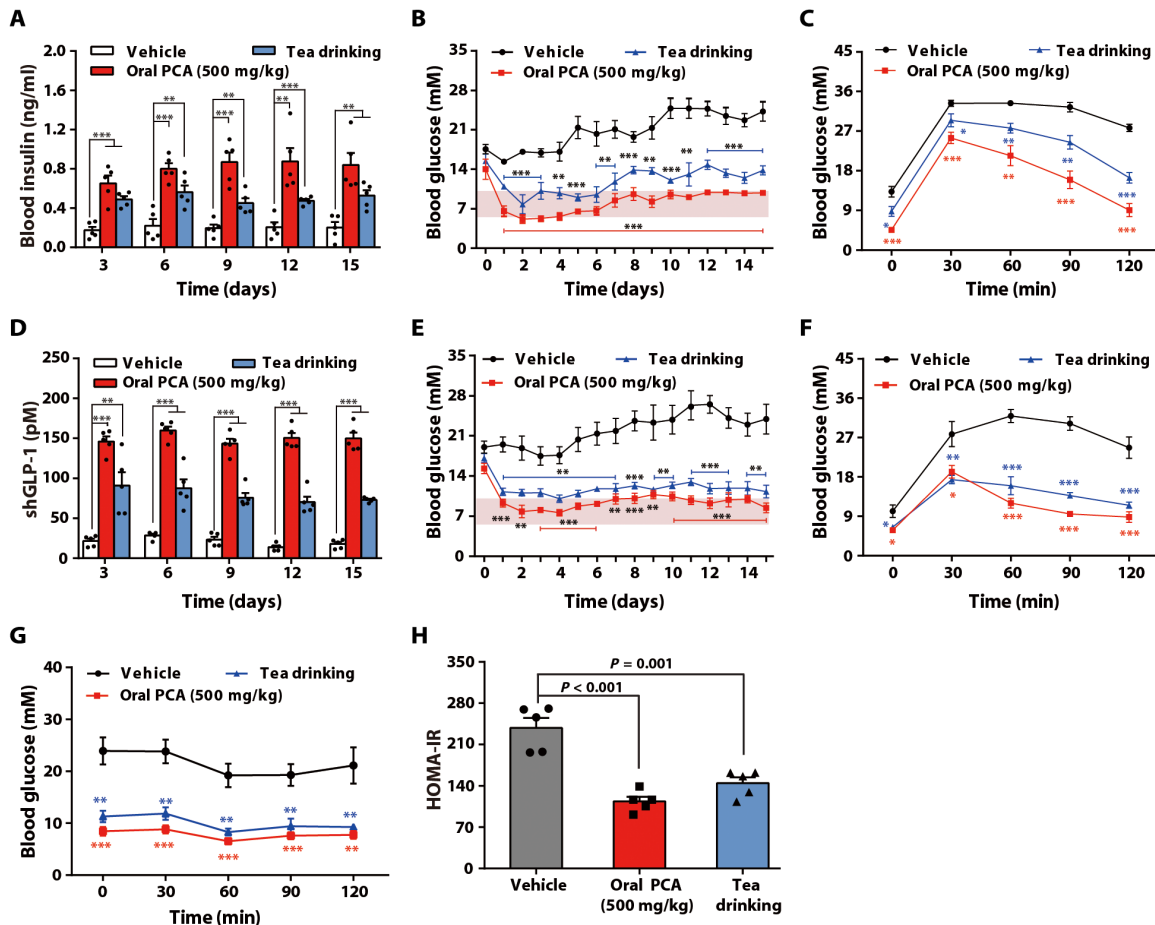


Fig. 6. PCA_{ON}-2.0 switch-controlled treatment of type 1 and type 2 diabetic mice achieved with orally infused PCA or tea drinking. (A to C) PCA_{ON}-2.0 switch-mediated treatment of type 1 diabetic mice. Type 1 diabetic mice implanted with 4×10^6 microencapsulated HEK_{PCA-2.0-SEAP-P2A-mINS} cells (200 cells per capsule) received oral administration of concentrated green tea ($900 \mu\text{l mouse}^{-1} \text{day}^{-1}$) or PCA ($500 \text{ mg kg}^{-1} \text{day}^{-1}$) thrice daily. Control mice were treated with water ($900 \mu\text{l mouse}^{-1} \text{day}^{-1}$). (A) Blood insulin and (B) blood glucose were profiled for 15 days after implantation. (C) Intraperitoneal glucose tolerance test was conducted on day 15 after implantation. (D to H) PCA_{ON}-2.0 switch-mediated treatment of type 2 diabetic mice. Type 2 diabetic mice implanted with 4×10^6 microencapsulated HEK_{PCA-2.0-shGLP-1-SEAP} cells (200 cells per capsule) received oral administration of the concentrated green tea ($900 \mu\text{l mouse}^{-1} \text{day}^{-1}$) or PCA ($500 \text{ mg kg}^{-1} \text{day}^{-1}$) thrice daily. Control mice were treated with water ($900 \mu\text{l mouse}^{-1} \text{day}^{-1}$). (D) Blood shGLP-1 and (E) blood glucose were profiled for 15 days after implantation. (F) Intraperitoneal glucose tolerance test and (G) insulin tolerance test were conducted on days 16 and 15, respectively, after implantation. (H) Insulin resistance was analyzed on day 12 after implantation. Pink area represents normal blood glucose range. All data represent the mean \pm SEM; two-tailed Student's *t* test, $n = 5$ mice. * $P < 0.05$, ** $P < 0.01$, *** $P < 0.001$ versus control. All individual-level data are in data file S2.

Relative to mice, the greater genetic, anatomical, and physiological similarity of nonhuman primates (NHPs) to humans makes them superior experimental disease models, especially for the development of engineered cell-based therapeutic strategies (38). We tested the applicability of the PCA_{ON} switch 1.0 to NHPs by implanting microencapsulated HEK_{PCA-ON-SEAP-P2A-mINS} cells into cynomolgus monkeys (Fig. 7A). We initially monitored SEAP in the bloodstream to determine suitable PCA administration dosages ($150 \text{ mg kg}^{-1} \text{day}^{-1}$) and implant sizes (3.7×10^7 cells/kg) to enable PCA_{ON} switch activity (Fig. 7B); we then administered a single injection of streptozotocin (100 mg/kg), thereby establishing an NHP model for type 1 diabetes mellitus. Subsequent daily PCA injections restored blood insulin (0.2 to 0.4 ng/ml), glucose homeostasis (5 to 10 mM) (Fig. 7, C and D), and intravenous glucose tolerance (Fig. 7, E and F).

Having determined that our PCA_{ON} switch 2.0 was substantially more sensitive (Figs. 5 and 6) and hoping to achieve similar control

of diabetes via oral dosing of PCA in the NHP model, we undertook a second series of experiments in which microencapsulated HEK_{PCA-ON-2.0-SEAP-P2A-shGLP-1} cells (3.7×10^7 cells/kg) were implanted intraperitoneally into a spontaneously developed type 2 diabetic cynomolgus monkey under anesthesia (Fig. 8A). Similar to the treatment efficacy with that observed in the type 2 diabetic mice, the daily oral administration of PCA ($150 \text{ mg kg}^{-1} \text{day}^{-1}$) rapidly increased shGLP-1 expression (60 to 120 pM) (Fig. 8B) and restored glucose homeostasis (reduced to 8 to 12 mM) (Fig. 8C), as well as the intravenous glucose tolerance (Fig. 8, D and E) in the diabetic monkeys. Moreover, the insulin sensitivity of the monkeys receiving oral PCA improved in 2 weeks (Fig. 8F). In both type 1 and type 2 diabetic monkeys, the blood biochemical indices that related to inflammatory responses, including white blood cell count, lymphocytes, monocytes, eosinophils, and basophils, did not increase at any point during the treatment compared with pretreatment (tables S1 and S2), indicating

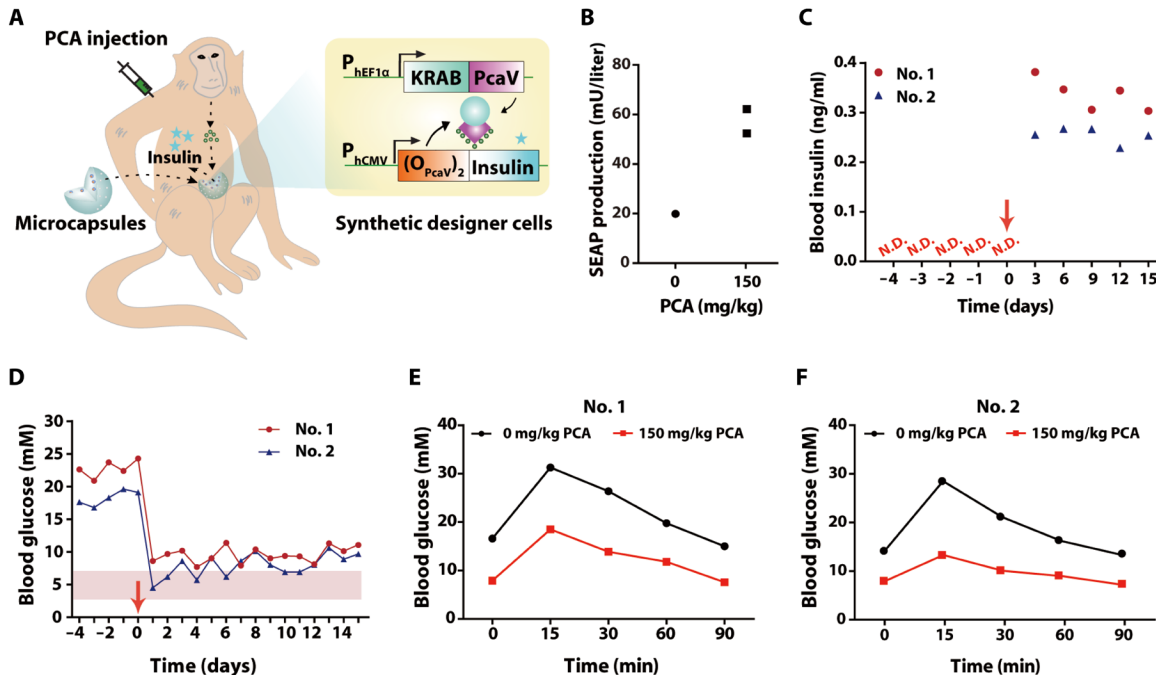


Fig. 7. PCA_{ON-1.0} switch-controlled treatment of type 1 diabetic NHPs. (A) Schematic of PCA-controlled cell-based therapy in monkeys. After administration of PCA, implanted microcapsules containing PCA-controlled engineered cells produce secreted protein therapeutics into the bloodstream of cynomolgus monkeys. (B) Validation of the PCA_{ON} system in monkeys. Cynomolgus monkeys were intraperitoneally implanted with 1.5×10^8 microencapsulated HEK-293_{PCA-ON-SEAP-P2A-mINS} cells (200 cells per capsule) and received thrice daily PCA injections ($150 \text{ mg kg}^{-1} \text{ day}^{-1}$). The control monkey received PBS instead of PCA. SEAP expression in the bloodstream of monkeys was profiled at 48 hours after implantation. SEAP expression in the bloodstream of individual monkeys was represented as dot plots. (C to F) PCA-dependent treatment of type 1 diabetic monkeys. Two type 1 diabetic monkeys (no. 1 and no. 2) were intraperitoneally implanted with 1.5×10^8 microencapsulated HEK_{PCA-ON-SEAP-P2A-mINS} cells and received thrice daily PCA injections ($150 \text{ mg kg}^{-1} \text{ day}^{-1}$). (C) Blood insulin and (D) glucose were profiled over a 4-day preimplantation and 15-day postimplantation period. N.D., not detectable. Red arrows represent the time of microcapsule implantation. Pink area represents normal blood glucose range. (E and F) Intravenous glucose tolerance of no. 1 and no. 2 monkeys was analyzed on day 5 after implantation. All individual-level data are in data file S2.

negligible local inflammatory responses. Moreover, blood biochemistry tests for evaluating liver and kidney functions showed an absence of major organ impairment during the treatment (tables S1 and S2).

DISCUSSION

We have developed a highly sensitive engineered cell system triggered by oral dosages of a common beverage for control of one of the most prevalent metabolic diseases. Although there have not yet been pre-clinical studies for the application of engineered cell-based therapies in humans, this first-in-monkey study demonstrates the feasibility of safely and successfully scaling up a treatment strategy by controlling microencapsulated engineered cells to release therapeutic outputs from animals such as mice to larger NHPs. Therefore, this study substantiates the medical utility of concepts developed in synthetic biology.

Green tea has been an extremely popular beverage for more than 2000 years. However, the medical potential of tea consumption has remained largely underestimated. As synthetic engineered cell therapies move into the clinic (41–43), we anticipate that user (patient) experiences will receive increasing attention. Some therapies will require the long-term delivery of trigger molecules (11, 44, 45), and we suspect that the attractive source of PCA represented by green tea drinking will be considered safe and will help to improve and encourage patient compliance. The ability to use a safe and common dietary molecule with antioxidant properties such as PCA offers a new strategy for

thinking about how to sustainably and flexibly activate therapeutic gene expression in long-term replacement therapies. Such therapies are generally designed to correct for various types of cell-function deficiencies or to control the precise drug delivery in long-term treatment regimens.

The control system devices that we have demonstrated in this study constitute a highly flexible control platform. We envision that it can be creatively deployed to solve a large variety of genetic control system problems in biology and biomedicine. It bears emphasis that we were able to use these new tools to implement an unprecedented U6 promoter–driven gRNA expression–mediated module to control CRISPR-Cas9 gene editing. We anticipate that it has potential capability of controlling outputs such as drug-delivery kinetics. Moreover, its ability will enable new molecular strategies relevant to both basic mechanistic studies and therapeutic contexts. For instance, our NIMPLY, AND, OR, and NOR logic gates were fully functional when mice received different combinations of PCA and VA; therefore, they can be used to constitute a feasible system for implementing complex therapeutic programs in the clinic. Moreover, the decision space defined by our five-gate implantable biocomputer should enable basic life science researchers to experimentally “program” elaborate and context-specific cellular outcomes for high-resolution mechanistic studies.

In this work, the second enhanced version of PCA_{ON} switch 2.0 was further developed by integrating a PCA pump into engineered cells to increase the sensitivity of the switch and finally achieve oral

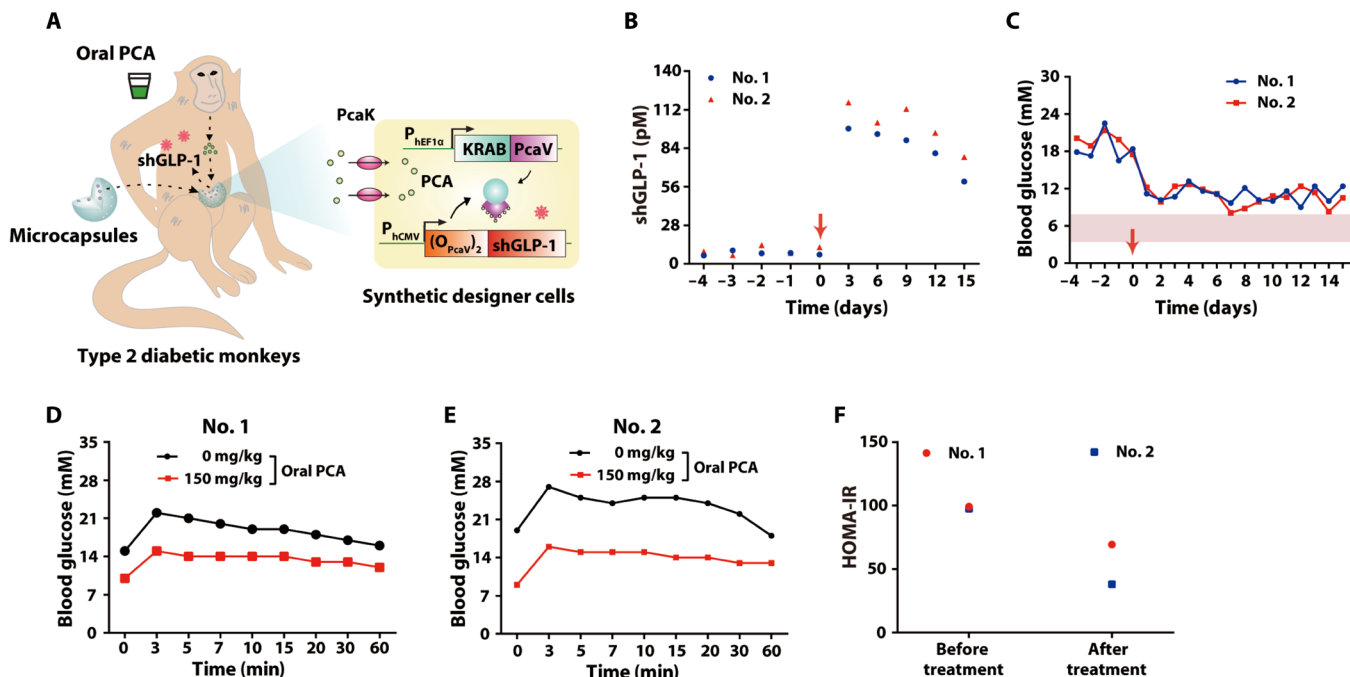


Fig. 8. PCA_{ON-2.0} switch-controlled treatment of type 2 diabetic NHPs achieved with oral administration of PCA. (A) Schematic of PCA_{ON-2.0} switch-controlled cell-based therapy in type 2 diabetic monkeys. After administration of PCA, implanted microcapsules containing PCA_{ON-2.0} switch-controlled engineered cells produce shGLP-1 into the bloodstream of cynomolgus monkeys. (B to F) PCA-dependent treatment of type 2 diabetic monkeys. Two type 2 diabetic monkeys were intraperitoneally implanted with 2.5×10^8 microencapsulated HEK_{PCA-2.0-shGLP-1-P2A-SEAP} cells and oral administration of thrice daily PCA solution ($150 \text{ mg kg}^{-1} \text{ day}^{-1}$). (B) Blood shGLP-1 and (C) glucose were profiled over a 4-day preimplantation and 15-day postimplantation period. Red arrows represent the time of microcapsule implantation. Pink area represents normal blood glucose range. (D and E) Intravenous glucose tolerance of no. 1 and no. 2 monkeys was analyzed on day 5 after implantation. (F) Insulin resistance was analyzed on day 12 after implantation. All individual-level data are in data file S2.

dosage of PCA or concentrated green tea to control blood glucose homeostasis in animals. The PCA_{ON} switch 2.0 remains exclusively sensitive to highly concentrated green tea (equivalent to $2.1 \text{ to } 6.3 \text{ mg mouse}^{-1} \text{ day}^{-1}$ of total tea polyphenols) and could not be triggered by usual tea drinking, indicating that the switch is safe and cannot be triggered by amounts of polyphenols or PCA in normal diet. We believe that there is still room to further improve the sensitivity of the PCA switch so as to make therapeutic outputs more controllable and the tea drinking program more achievable. For example, it is possible to obtain a more sensitive mutated transcriptional repressor PcaV by protein-directed evolution technology.

It is essential to overcome the key issue of the therapeutic efficacy and unpredictable safety issues when upscaling engineered cell-based therapies toward larger animals (46, 47). The present study shows that engineered cell-based therapies can retain full therapeutic potency when they are translated from mice to NHPs. An increase in the implant size (the number of microencapsulated engineered cells) was sufficient to recapitulate the antidiabetic treatment from mice to monkeys with no significant adverse effects. PCA, a major metabolite of antioxidant polyphenols from green tea (48), is known to be metabolically inert and known to rapidly enter the bloodstream and be renally cleared within 8 hours in mice (49). With its metabolic inertness, rapid absorption, and clearance rate, PCA seems to be a particularly suitable trigger molecule for clinical applications. In addition, we showed that implanted PCA_{ON}-carrying engineered cells could be activated when mice drank highly concentrated green tea, showing that a future scenario of lifestyle-adapted cell-based therapies is feasible.

However, there are limitations to the current PCA-inducible engineered cells to be used for translational purposes. The PCA_{ON} switch was stably integrated into the genome by the Sleeping Beauty transposon system. Because of a random integration, unwanted insertional mutagenesis might occur. Therefore, gene editing tools, such as CRISPR, could be used to enable facile and permanent integration of the switch into the targeted genomic sequences in human cells without insertional mutagenesis. The chassis of the HEK-293 cells are easily handled, transfected, and compatible to the PCA_{ON} switch. For translational applications, they must also be safe (no side effects) in humans. Hence, autologous parental cells from patients' own mesenchymal stem cells may provide immunocompatible and noncarcinogenic autologous or allogeneic cell sources. The lifespan of the engineered cells inside the alginate microcapsules is an imperative issue. The encapsulation technology also needs to be further improved, which is a major challenge in realizing long-term cell therapy.

Collectively, our work shows how beverage phenolic acid-controlled switches can expand the toolbox of mammalian synthetic biology. This work demonstrates a safe, robust, and convenient strategy for the dynamic remote control of therapeutic outputs for future gene- and cell-based precision medicine applications.

MATERIALS AND METHODS

Study design

The main goal of our study was to create a green tea-triggered genetic control system as a multifunctional platform for genome and epigenome engineering, engineered cell biocomputer implants

for Boolean calculations in live animals, and diabetes therapy in both mice and monkeys. We developed PCA (a green tea metabolite)-controlled gene switches by assembling an *S. coelicolor*-derived transcriptional repressor to eukaryotic epigenetic effectors. After optimizing and validating the PCA_{ON} switch in HEK-293 cells, we generated a stably transgenic HEKPCA-ON-P2A-SEAP cell line for testing the long-term transgene expression kinetics in vivo. To achieve the remote control of gene editing and epigenetic remodeling in a PCA-dependent manner, we capitalized on the regulatory module of the PCA_{ON} switch to engineer and validate three PCA-inducible CRISPR-Cas9 systems for the gRNA-dependent inhibition (PcaRi), activation (PcaRa), and deletion (PcaRdel) of endogenous genes in human cells. Quantitative polymerase chain reaction (qPCR) analysis and mismatch-sensitive T7E1 assay were used to examine the expression of endogenous genes and the efficiency of gene editing, respectively. To create food phenolic acid-controlled biocomputers in live animals, we implanted microencapsulated cells performing various logic operations into mice and administered PCA and VA in various combinations. To test the potential of the PCA_{ON} system for treating experimental diabetes, we generated two stably transgenic HEK_{PCA-ON-SEAP-P2A-mINS} and HEK_{PCA-ON-shGLP-1-P2A-SEAP} cell lines expressing insulin and shGLP-1 in a PCA-dependent manner, respectively. For in vivo experiments, 12-week-old male db/db mice (BKS.Cg-Dock7m^{+/+} Leprd/J, derived from C57BL/6J mice, Charles River Laboratory) were chosen as a disease model for type 2 diabetes. Both type 1 diabetic mouse and monkey models were created for this study as well, which is described in the Supplementary Materials. To achieve oral infusion of PCA or green tea to treat diabetes, we further developed an improved PCA_{ON} switch 2.0. Two stably isogenic cell clones HEK_{PCA-ON-2.0-SEAP-P2A-mINS} and HEK_{PCA-ON-2.0-shGLP-1-P2A-SEAP} were further selected for cell-based diabetes therapy in mice and monkeys. To assess the safety of diabetes therapy in monkeys, blood samples were collected for complete blood count (CBC) and blood biochemistry test. All in vitro experiments were done in triplicate. In all experiments, mice were randomly assigned to individual groups of five to six mice. The experimenter was blinded to the analysis of all samples. Neither animals nor samples were excluded from the study.

Cloning and vector construction

Comprehensive design and construction details for all expression plasmids are provided in table S3. The detailed DNA sequence information of the most important plasmids used in this study is provided in data file S1. Some expression vectors were cloned by Gibson assembly according to the manufacturer's instructions [Seamless Assembly Cloning Kit, Obio Technology Inc., catalog no. BACR(C)20144001]. All cloned genetic components have been confirmed by sequencing (Genewiz Inc.).

Cell transfection

All cells were transfected with an optimized polyethyleneimine (PEI)-based protocol. Briefly, 5×10^4 cells seeded per well of a 24-well plate 18 hours before transfection were incubated for 6 hours with 50 μ l of a 3:1 PEI: DNA mixture (w/w) (PEI; molecular weight, 25,000; stock solution, 1 mg/ml in ddH₂O; Polysciences, catalog no. 24765) containing 0.2 to 0.6 μ g of total DNA in serum- and antibiotic-free Dulbecco's modified Eagle's medium (DMEM). The transfection mixture and cells could be scaled up to 12-well plates, 6-well plates, or 10- or 15-cm culture dishes. The total amounts of DNA and

transfection reagent were scaled up accordingly as well. Cell titers and viability were quantified with a Countess II automated cell counter (Life Technologies).

Analytical assays

SEAP reporter assay

The production of human placental SEAP in cell culture supernatants was quantified using a *p*-nitrophenylphosphate-based light absorbance time course assay, as described previously (50). Briefly, 120 μ l of substrate solution [100 μ l of 2x SEAP buffer containing 20 mM homoarginine, 1 mM MgCl₂, and 21% (vol/vol) diethanolamine] (pH 9.8) and 20 μ l of substrate solution containing 120 mM *p*-nitrophenylphosphate were added to 80 μ l of heat-inactivated (65°C, 30 min) cell culture supernatant. The time course of absorbance at 405 nm was measured at 37°C by using a Synergy H1 hybrid multimode microplate reader (BioTek Instruments Inc.) with Gen5 software (version 2.04). Quantification of SEAP production was calculated from the slope of the time-dependent increase in light absorbance. The SEAP production in mouse or monkey serum was profiled using a chemiluminescence-based assay kit (Roche Diagnostics, catalog no. 11779842001) according to the manufacturer's protocol.

qPCR analysis

Total RNA from cells was harvested using an RNAiso Plus Kit (Takara Bio, catalog no. 9108) according to the manufacturer's instructions. A total of 1 μ g of RNA was reverse-transcribed into cDNA using a PrimeScript RT Reagent Kit with the gDNA Eraser (Takara Bio, catalog no. RR047) according to the manufacturer's protocol. qPCR analysis was performed on a Real-Time PCR Instrument (QuantStudio 3, Thermo Fisher Scientific Inc.) using SYBR Premix Ex Taq (Takara Bio, catalog no. RR420) for detecting each target gene; primer sequences are detailed in table S4. The relative cycle threshold (CT) was determined and normalized against the endogenous housekeeping gene glyceraldehyde 3-phosphate dehydrogenase. The results were expressed as a relative mRNA amount using the standard $\Delta\Delta Ct$ method.

Mismatch-sensitive T7E1 assay

sgRNA-targeted genomic region was PCR-amplified using the primers detailed in table S5. Briefly, 20 μ l of mixture containing 2 μ l of 10 \times M buffer (Takara Bio) and 500 ng of purified PCR amplicons was reannealed to form heteroduplex DNA and then 0.3 μ l of T7 endonuclease I (New England BioLabs, catalog no. M0302) was added. Two hours after incubation at 37°C, the digested products were analyzed by 2 to 2.5% agarose gel electrophoresis. The percentage of indel mutation by Cas9 was calculated with the following formula: Indel (%) = $100 \times (1 - (1 - (b + c)/(a + b + c))^{1/2})$, where a is the intensity of undigested PCR amplicon and b and c are the intensities of the T7E1-digested products.

Mouse experiments

Microcapsule implants in mice

Intraperitoneal implants were prepared by encapsulating transgenic HEK-293 cells into coherent alginate-poly-(L-lysine)-alginate beads (400 μ m; 200 cells per capsule) using a B-395 Pro encapsulator (BÜCHI Labortechnik AG) set to the following parameters: a 200- μ m nozzle with a vibration frequency of 1300 Hz, a 25-ml syringe operated at a flow rate of 450 U, and 1.10-kV voltage for bead dispersion. Twelve-week-old male wild-type C57BL/6J mice [East China Normal University (ECNU) Laboratory Animal Centre], 12-week-old male type 1 diabetic mice, or 12-week-old male db/db mice (BKS.Cg-Dock7m^{+/+} Lepr^{db}/J, derived from

C57BL/6J mice, Charles River Laboratories) were intraperitoneally injected with 800 μ l of DMEM containing 2×10^6 to 4×10^6 microencapsulated engineered human cells (200 transgenic HEK-293 cells per capsule). Control compounds (green tea extracts or PCA) were prepared and administered orally or via injection at 1 hour (at the earliest) after implantation. Blood samples were collected via centrifugation (2700g, 10 min) of clotted blood (37°C for 0.5 hours and then 4°C for 2 hours) at different time periods after implantation.

Logic computations in mice

According to the PEI-based plasmid transfection protocol, 1×10^7 HEK-293 cells seeded in a 15-cm culture dish were incubated with a total of 18 μ g of plasmid DNA mixture (the detailed transfection mixtures for each logic gate are provided in table S6). Six hours after incubation, the transfected cells were further cultured in fresh culture media for 4 hours before harvested for encapsulation. Microencapsulated cells containing logic gates were intraperitoneally implanted into the wild-type C57BL/6J mice. After implantation, the mice received thrice daily injections of PCA or VA or both of the two compounds. Control were collected for quantification of SEAP expression 48 hours after implantation.

NHP experiments

Microcapsule implantation in type 1 and type 2 diabetic monkeys
The type 1 diabetic monkeys were anesthetized with ketamine hydrochloride (10 mg/kg; Bucolic, Jiangsu Beikang Pharmacy Co. Ltd.), followed by a slow intraperitoneal injection of 60 ml of DMEM containing 1.5×10^8 microencapsulated HEK-293PCA-ON-SEAP-P2A-mINS cells (3.7×10^7 cells/kg; 200 cells per capsule) under the guidance of the B-ultrasound scanner (MyLabOne, Esaote S.P.A.). After implantation, the monkeys were intraperitoneally injected with PCA thrice daily (150 mg kg $^{-1}$ day $^{-1}$). The fasting blood glucose in the morning was recorded every day with a Contour Glucometer (OneTouch UltraEasy, Johnson & Johnson Medical Ltd.).

Similarly, the type 2 diabetic monkeys were anesthetized and then followed by a slow intraperitoneal injection of 100 ml of DMEM containing 2.5×10^8 microencapsulated HEK_{PCA-ON-2.0-shGLP-1-P2A-SEAP} cells (3.7×10^7 cells/kg; 200 cells per capsule) under the guidance of the B-ultrasound scanner. After implantation, the monkeys were orally delivered with PCA thrice daily (150 mg kg $^{-1}$ day $^{-1}$). The fasting blood glucose in the morning was recorded every day with a Roche Accu-Chek Performa handheld glucometer.

CBC in monkeys

Blood specimens were collected into EDTAK₂ anticoagulant tubes (Sanli Medical Technology Development Co. Ltd.) (51). Each specimen was performed on the Sysmex XE-2100 automated hematology analyzer (Sysmex Corporation) within 8 hours of collection. Measured CBC parameters included white blood cell count, red blood cell count, mean platelet volume, lymphocytes, monocytes, eosinophils, and basophils.

Blood biochemistry test in monkeys

Fasting blood specimens were collected into separate tubes (Sanli Medical Technology Development Co. Ltd.) (52). Each specimen was analyzed by Beckman Coulter DXC 800 (Synchron, Beckman Coulter Inc.) within 8 hours of collection. Measured biochemistry parameters for liver function included total protein, globulin, direct bilirubin, and total bile acid. Measured biochemistry parameters for kidney function contained blood urea nitrogen, carbon dioxide combining power, and cystatin C.

Ethics statement

All experiments involving mice were performed according to the protocol approved by the ECNU Animal Care and Use Committee (protocol IDs: m20140301 and m20190801). Experiments involving handling and care of type 1 diabetic monkeys were in compliance with the guidelines approved by Guangdong Landao Biotechnology Co. Ltd., and the protocol was approved by the Shenzhen Second People's Hospital Animal Care and Use Committee (protocol ID: LLSC2017070607). All the procedures related to handling, care, and treatment of the type 2 diabetic monkeys in this study were performed according to the guidelines approved by the Association for Assessment and Accreditation of Laboratory Animal Care. All the procedures for sample or data collection used in the type 2 diabetic monkey study were approved by the Institutional Animal Care and Use Committee (protocol ID: AN-1803-05-17) (Crown Bioscience Inc.). All animal experiments were carried out in accordance with the Ministry of Science and Technology of the People's Republic of China on Animal Care Guidelines. All mice were euthanized after the termination of the experiments.

Quantification and statistical analysis

All in vitro data represent means \pm SD of three independent experiments. For the mouse experiments, each treatment group consisted of randomly selected mice ($n = 5$ to 6). The blood sample analysis was blinded. Comparisons between groups were performed using Student's *t* tests, and the results are expressed as means \pm SEM. Differences were considered statistically significant at $P < 0.05$. Prism 5 software (version 5.01, GraphPad Software Inc.) was used for statistical analysis.

SUPPLEMENTARY MATERIALS

stm.scienmag.org/cgi/content/full/11/515/eaav8826/DC1

Materials and Methods

- Fig. S1. Assessment of PCA-mediated toxicity on HEK-293 cells.
- Fig. S2. Optimization of the PCA_{ON} system in HEK-293 cells.
- Fig. S3. PCA analog-mediated SEAP expression in pJY14/pJY29-transgenic HEK-293 cells.
- Fig. S4. PCA_{ON}-dependent SEAP expression kinetics in HEK-293 cells.
- Fig. S5. Design, construction, and optimization of the PcaR-mediated inhibition device (PcaRi) for gene inhibition.
- Fig. S6. Design, construction, and optimization of the PcaR-mediated activation device (PcaRa) for gene activation.
- Fig. S7. Schematics of a synthetic PcaR-mediated gene deletion device (PcaRdel).
- Fig. S8. Controls with constitutively active CRISPR-dCas9 device-mediated genome repression and activation.
- Fig. S9. PCA- and VA-controlled programmable biocomputers in mammalian cells.
- Fig. S10. Flow cytometric histograms showing input-triggered single-cell d2EYFP expression of all programmed logic circuits.
- Fig. S11. Validation of the VA_{ON} and the VA_{OFF} system in mammalian cells.
- Fig. S12. Validation of the PCA_{OFF} system in mammalian cells.
- Fig. S13. Construction and characterization of the stable cell lines.
- Fig. S14. PCA_{ON-2.0} switch-controlled treatment in type 1 diabetic mice by oral delivery of PCA.
- Fig. S15. Hypoglycemic effect on type 1 and type 2 diabetic mice by oral administration of PCA or tea drinking.
- Table S1. The CBC and blood biochemistry tests in type 1 diabetic monkeys.
- Table S2. The CBC and blood biochemistry tests in type 2 diabetic monkeys.
- Table S3. Plasmids designed and used in this study.
- Table S4. The primers used for qPCR analysis.
- Table S5. The primers used for PCR amplification.
- Table S6. The expression vectors and mixtures for logic gates in mice.
- Table S7. The expression vectors and mixtures for logic gates in mammalian cells.
- Data file S1. DNA sequence information of plasmids used in this study.
- Data file S2. Individual subject-level data.
- References (53–64)
- [View/request a protocol for this paper from Bio-protocol.](#)

REFERENCES AND NOTES

- N. M. E. Fogarty, A. McCarthy, K. E. Snijders, B. E. Powell, N. Kubikova, P. Blakeley, R. Lea, K. Elder, S. E. Wamaitha, D. Kim, V. Maciulyte, J. Kleinjung, J.-S. Kim, D. Wells, L. Vallier, A. Bertero, J. M. A. Turner, K. K. Niakan, Genome editing reveals a role for OCT4 in human embryogenesis. *Nature* **550**, 67–73 (2017).
- B. Zetsche, S. E. Volz, F. Zhang, A split-Cas9 architecture for inducible genome editing and transcription modulation. *Nat. Biotechnol.* **33**, 139–142 (2015).
- I. B. Hilton, A. M. DiPippo, C. M. Vockley, P. I. Thakore, G. E. Crawford, T. E. Reddy, C. A. Gersbach, Epigenome editing by a CRISPR-Cas9-based acetyltransferase activates genes from promoters and enhancers. *Nat. Biotechnol.* **33**, 510–517 (2015).
- S. M. G. Braun, J. G. Kirkland, E. J. Chory, D. Husmann, J. P. Calarco, G. R. Crabtree, Rapid and reversible epigenome editing by endogenous chromatin regulators. *Nat. Commun.* **8**, 560 (2017).
- D. Ausländer, S. Ausländer, X. Pierrat, L. Hellmann, L. Rachid, M. Fussenegger, Programmable full-adder computations in communicating three-dimensional cell cultures. *Nat. Methods* **15**, 57–60 (2018).
- A. A. Green, J. Kim, D. Ma, P. A. Silver, J. J. Collins, P. Yin, Complex cellular logic computation using ribocomputing devices. *Nature* **548**, 117–121 (2017).
- M. Xie, H. Ye, H. Wang, G. Charpin-El Hamri, C. Lormeau, P. Saxena, J. Stelling, M. Fussenegger, β -Cell-mimetic designer cells provide closed-loop glycemic control. *Science* **354**, 1296–1301 (2016).
- J. Shao, S. Xue, G. Yu, Y. Yu, X. Yang, Y. Bai, S. Zhu, L. Yang, J. Yin, Y. Wang, S. Liao, S. Guo, M. Xie, M. Fussenegger, H. Ye, Smartphone-controlled optogenetically engineered cells enable semiautomatic glucose homeostasis in diabetic mice. *Sci. Transl. Med.* **9**, eaal2298 (2017).
- L. Nissim, M.-R. Wu, E. Pery, A. Binder-Nissim, H. I. Suzuki, D. Stupp, C. Wehrspaun, Y. Tabach, P. A. Sharp, T. K. Lu, Synthetic RNA-based immunomodulatory gene circuits for cancer immunotherapy. *Cell* **171**, 1138–1150.e15 (2017).
- K. T. Roybal, J. Z. Williams, L. Morsut, L. J. Rupp, I. Kolinko, J. H. Choe, W. J. Walker, K. A. McNally, W. A. Lim, Engineering T cells with customized therapeutic response programs using synthetic notch receptors. *Cell* **167**, 419–432.e16 (2016).
- C.-Y. Wu, K. T. Roybal, E. M. Puchner, J. Onuffer, W. A. Lim, Remote control of therapeutic T cells through a small molecule-gated chimeric receptor. *Science* **350**, aab4077 (2015).
- K. T. Roybal, W. A. Lim, Synthetic immunology: Hacking immune cells to expand their therapeutic capabilities. *Annu. Rev. Immunol.* **35**, 229–253 (2017).
- R. M. Dudek, Y. Chuang, J. N. Leonard, Engineered cell-based therapies: A vanguard of design-driven medicine. *Adv. Exp. Med. Biol.* **844**, 369–391 (2014).
- F. Lienert, J. J. Lohmueller, A. Garg, P. A. Silver, Synthetic biology in mammalian cells: Next generation research tools and therapeutics. *Nat. Rev. Mol. Cell Biol.* **15**, 95–107 (2014).
- S. Urlinger, U. Baron, M. Thellmann, M. T. Hasan, H. Bujard, W. Hillen, Exploring the sequence space for tetracycline-dependent transcriptional activators: Novel mutations yield expanded range and sensitivity. *Proc. Natl. Acad. Sci. U.S.A.* **97**, 7963–7968 (2000).
- R. Chait, A. C. Palmer, I. Yelin, R. Kishony, Pervasive selection for and against antibiotic resistance in inhomogeneous multistress environments. *Nat. Commun.* **7**, 10333 (2016).
- S. Valentin, A. Morales, J. L. Sánchez, A. Rivera, Safety and efficacy of doxycycline in the treatment of rosacea. *Clin. Cosmet. Investig. Dermatol.* **2**, 129–140 (2009).
- M. Gitzinger, C. Kemmer, D. A. Fluri, M. D. El-Baba, W. Weber, M. Fussenegger, The food additive vanillic acid controls transgene expression in mammalian cells and mice. *Nucleic Acids Res.* **40**, e37 (2012).
- M. Xie, H. Ye, G. Charpin-El Hamri, M. Fussenegger, Antagonistic control of a dual-input mammalian gene switch by food additives. *Nucleic Acids Res.* **42**, e116 (2014).
- M. Gitzinger, C. Kemmer, M. D. El-Baba, W. Weber, M. Fussenegger, Controlling transgene expression in subcutaneous implants using a skin lotion containing the apple metabolite phloretin. *Proc. Natl. Acad. Sci. U.S.A.* **106**, 10638–10643 (2009).
- D. Mischek, C. Krapfenbauer-Cermak, Exposure assessment of food preservatives (sulphites, benzoic and sorbic acid) in Austria. *Food Addit. Contam. Part A Chem. Anal. Control Expo. Risk Assess.* **29**, 371–382 (2012).
- S. Ausländer, M. Fussenegger, Engineering gene circuits for mammalian cell-based applications. *Cold Spring Harb. Perspect. Biol.* **8**, a023895 (2016).
- D. Bojar, L. Scheller, G. Charpin-El Hamri, M. Xie, M. Fussenegger, Caffeine-inducible gene switches controlling experimental diabetes. *Nat. Commun.* **9**, 2318 (2018).
- C. S. Yang, X. Wang, G. Lu, S. C. Picinich, Cancer prevention by tea: Animal studies, molecular mechanisms and human relevance. *Nat. Rev. Cancer* **9**, 429–439 (2009).
- M. A. Ferreira, D. M. Silva, A. C. de Morais Jr., J. F. Mota, P. B. Botelho, Therapeutic potential of green tea on risk factors for type 2 diabetes in obese adults—A review. *Obes. Rev.* **17**, 1316–1328 (2016).
- T. M. Haqqi, D. D. Anthony, S. Gupta, N. Ahmad, M.-S. Lee, G. K. Kumar, H. Mukhtar, Prevention of collagen-induced arthritis in mice by a polyphenolic fraction from green tea. *Proc. Natl. Acad. Sci. U.S.A.* **96**, 4524–4529 (1999).
- L. Hartley, N. Flowers, J. Holmes, A. Clarke, S. Stranges, L. Hooper, K. Rees, Green and black tea for the primary prevention of cardiovascular disease. *Cochrane Database Syst. Rev.* **2013**, CD009934 (2013).
- P. G. Pietta, P. Simonetti, C. Gardana, A. Brusamolino, P. Morazzoni, E. Bombardelli, Catechin metabolites after intake of green tea infusions. *Biofactors* **8**, 111–118 (1998).
- J. R. Davis, B. L. Brown, R. Page, J. K. Sello, Study of PcaV from *Streptomyces coelicolor* yields new insights into ligand-responsive MarR family transcription factors. *Nucleic Acids Res.* **41**, 3888–3900 (2013).
- D. P. Nguyen, Y. Miyaoka, L. A. Gilbert, S. J. Mayerl, B. H. Lee, J. S. Weissman, B. R. Conklin, J. A. Wells, Ligand-binding domains of nuclear receptors facilitate tight control of split CRISPR activity. *Nat. Commun.* **7**, 12009 (2016).
- Y. Nihongaki, F. Kawano, T. Nakajima, M. Sato, Photoactivatable CRISPR-Cas9 for optogenetic genome editing. *Nat. Biotechnol.* **33**, 755–760 (2015).
- J. G. Zalatana, M. E. Lee, R. Almeida, L. A. Gilbert, E. H. Whitehead, M. La Russa, J. C. Tsai, J. S. Weissman, J. E. Dueber, L. S. Qi, W. A. Lim, Engineering complex synthetic transcriptional programs with CRISPR RNA scaffolds. *Cell* **160**, 339–350 (2015).
- S. Konermann, M. D. Brigham, A. E. Trevino, J. Joung, O. O. Abudayyeh, C. Barcena, P. D. Hsu, N. Habib, J. S. Gootenberg, H. Nishimasu, O. Nureki, F. Zhang, Genome-scale transcriptional activation by an engineered CRISPR-Cas9 complex. *Nature* **517**, 583–588 (2015).
- S. W. Cho, S. Kim, J. M. Kim, J.-S. Kim, Targeted genome engineering in human cells with the Cas9 RNA-guided endonuclease. *Nat. Biotechnol.* **31**, 230–232 (2013).
- B. H. Weinberg, N. T. H. Pham, L. D. Caraballo, T. Lozano, A. Engel, S. Bhatia, W. W. Wong, Large-scale design of robust genetic circuits with multiple inputs and outputs for mammalian cells. *Nat. Biotechnol.* **35**, 453–462 (2017).
- J. Bonnet, P. Yin, M. E. Ortiz, P. Subsoontorn, D. Endy, Amplifying genetic logic gates. *Science* **340**, 599–603 (2013).
- S. Ausländer, D. Ausländer, M. Müller, M. Wieland, M. Fussenegger, Programmable single-cell mammalian biocomputers. *Nature* **487**, 123–127 (2012).
- J. C. Pickup, Insulin-pump therapy for type 1 diabetes mellitus. *N. Engl. J. Med.* **366**, 1616–1624 (2012).
- G. B. Parsons, D. W. Souza, H. Wu, D. Yu, S. G. Wadsworth, R. J. Gregory, D. Armentano, Ectopic expression of glucagon-like peptide 1 for gene therapy of type II diabetes. *Gene Ther.* **14**, 38–48 (2007).
- C. Pernstich, L. Senior, K. A. MacInnes, M. Forsaith, P. Curnow, Expression, purification and reconstitution of the 4-hydroxybenzoate transporter PcaK from *Acinetobacter* sp. ADP1. *Protein Expr. Purif.* **101**, 68–75 (2014).
- W. C. Ruder, T. Lu, J. J. Collins, Synthetic biology moving into the clinic. *Science* **333**, 1248–1252 (2011).
- T. Kitada, B. DiAndrea, B. Teague, R. Weiss, Programming gene and engineered-cell therapies with synthetic biology. *Science* **345**, eaad1067 (2018).
- M. Xie, M. Fussenegger, Designing cell function: Assembly of synthetic gene circuits for cell biology applications. *Nat. Rev. Mol. Cell Biol.* **19**, 507–525 (2018).
- J. Yue, X. Gou, Y. Li, B. Wicksteed, X. Wu, Engineered epidermal progenitor cells can correct diet-induced obesity and diabetes. *Cell Stem Cell* **21**, 256–263.e4 (2017).
- R. Sakemura, S. Terakura, K. Watanabe, J. Julamanee, E. Takagi, K. Miyao, D. Koyama, T. Goto, R. Hanajiri, T. Nishida, M. Murata, H. Kiyoi, A Tet-On inducible system for controlling CD19-chimeric antigen receptor expression upon drug administration. *Cancer Immunol. Res.* **4**, 658–668 (2016).
- N. Saito, H. Chono, H. Shibata, N. Agyeyama, Y. Yasutomi, J. Mineno, CD4⁺ T cells modified by the endoribonuclease MazF are safe and can persist in SHIV-infected rhesus macaques. *Mol. Ther. Nucleic Acids* **3**, e168 (2014).
- G. Orive, D. Emerich, A. Khademhosseini, S. Matsumoto, R. M. Hernández, J. L. Pedraz, T. Desai, R. Calafiore, P. de Vos, Engineering a clinically translatable bioartificial pancreas to treat type I diabetes. *Trends Biotechnol.* **36**, 445–456 (2018).
- S. Kakkar, S. Bais, A review on protocatechuic acid and its pharmacological potential. *ISRN Pharmacol.* **2014**, 952943 (2014).
- W. Chen, D. Wang, L.-s. Wang, D. Bei, J. Wang, W. A. See, S. R. Mallory, G. D. Stoner, Z. Liu, Pharmacokinetics of protocatechuic acid in mouse and its quantification in human plasma using LC-tandem mass spectrometry. *J. Chromatogr. B Analyt. Technol. Biomed. Life Sci.* **908**, 39–44 (2012).
- S. Xue, J. Yin, J. Shao, Y. Yu, L. Yang, Y. Wang, M. Xie, M. Fussenegger, H. Ye, A synthetic-biology-inspired therapeutic strategy for targeting and treating hepatogenous diabetes. *Mol. Ther.* **25**, 443–455 (2017).
- S. Nakayama, H. Koie, K. Kanayama, Y. Katai, Y. Ito-Fujishiro, T. Sankai, Y. Yasutomi, N. Agyeyama, Establishment of reference values for complete blood count and blood gases in cynomolgus monkeys (*Macaca fascicularis*). *J. Vet. Med. Sci.* **79**, 881–888 (2017).
- M.-L. Wu, L. Gong, C. Qian, Z.-G. Liang, W. Zeng, Characteristics of blood chemistry, hematology, and lymphocyte subsets in pregnant rhesus monkeys. *Chin. J. Nat. Med.* **13**, 409–414 (2015).
- L. Mátés, M. K. L. Chuah, E. Belay, B. Jerchow, N. Manoj, A. Acosta-Sánchez, D. P. Grzela, A. Schmitt, K. Becker, J. Matrai, L. Ma, E. Samara-Kuko, C. Gysemans, D. Pryputniewicz, C. Miskey, B. Fletcher, T. VandenDriessche, Z. Ivics, Z. Izsák, Molecular evolution

- of a novel hyperactive *Sleeping Beauty* transposase enables robust stable gene transfer in vertebrates. *Nat. Genet.* **41**, 753–761 (2009).
54. K. Slinkard, V. L. Singleton, Total phenol analysis: Automation and comparison with manual methods. *Am. J. Enol. Vitic.* **28**, 49–55 (1977).
 55. X. Wang, B. Wang, G. Sun, J. Wu, Y. Liu, Y. Wang, Y.-F. Xiao, Dysglycemia and dyslipidemia models in nonhuman primates: Part I. Model of naturally occurring diabetes. *J. Diabetes Metab.* **S13**, 10.4172/2155-6156.S13-010, (2015).
 56. B. C. Hansen, Investigation and treatment of type 2 diabetes in nonhuman primates. *Methods Mol. Biol.* **933**, 177–185 (2012).
 57. D. Ausländer, S. Ausländer, G. Charpin-El Hamri, F. Sedlmayer, M. Müller, O. Frey, A. Hierlemann, J. Stelling, M. Fussenegger, A synthetic multifunctional mammalian pH sensor and CO₂ transgene-control device. *Mol. Cell* **55**, 397–408 (2014).
 58. A. Casu, R. Bottino, A. N. Balamurugan, H. Hara, D. J. van der Windt, N. Campanile, C. Smetanka, D. K. C. Cooper, M. Trucco, Metabolic aspects of pig-to-monkey (*Macaca fascicularis*) islet transplantation: Implications for translation into clinical practice. *Diabetologia* **51**, 120–129 (2008).
 59. G. Sun, X. Wang, Y. Liu, B. Wang, G. Sun, K. Chng, Y.-F. Xiao, Y.-X. Wang, Effects of anesthesia on hyperglycemic and insulinotropic responses to intravenous glucose and mixed meal tolerance tests in cynomolgus monkeys with naturally occurring diabetes. *Int. J. Primatol. Res.* **1**, 001–009 (2017).
 60. Z. Hou, Y. Zhang, N. E. Propson, S. E. Howden, L.-F. Chu, E. J. Sontheimer, J. A. Thomson, Efficient genome engineering in human pluripotent stem cells using Cas9 from *Neisseria meningitidis*. *Proc. Natl. Acad. Sci. U.S.A.* **110**, 15644–15649 (2013).
 61. L. Cong, F. A. Ran, D. Cox, S. Lin, R. Barretto, N. Habib, P. D. Hsu, X. Wu, W. Jiang, L. A. Marraffini, F. Zhang, Multiplex genome engineering using CRISPR/Cas systems. *Science* **339**, 819–823 (2013).
 62. A. W. Cheng, H. Wang, H. Yang, L. Shi, Y. Katz, T. W. Theunissen, S. Rangarajan, C. S. Shivalila, D. B. Dadon, R. Jaenisch, Multiplexed activation of endogenous genes by CRISPR-on, an RNA-guided transcriptional activator system. *Cell Res.* **23**, 1163–1171 (2013).
 63. M. Fussenegger, S. Moser, X. Mazur, J. E. Bailey, Autoregulated multicistronic expression vectors provide one-step cloning of regulated product gene expression in mammalian cells. *Biotechnol. Prog.* **13**, 733–740 (1997).
 64. H. Ye, M. Xie, S. Xue, G. Charpin-El Hamri, J. Yin, H. Zulewski, M. Fussenegger, Self-adjusting synthetic gene circuit for correcting insulin resistance. *Nat. Biomed. Eng.* **1**, 0005 (2017).

Acknowledgments: We thank Z. Zou (Guangdong Landao Biotechnology Co. Ltd.) for help with the type 1 diabetic monkey experiments and Y. Liu and J. Zhang (Crown Bioscience, Inc.) for help with the type 2 diabetic monkey experiments. We also thank the ECNU Multifunctional Platform for Innovation (011) for supporting the mouse experiments.

Funding: This work was financially supported by grants from the National Key R&D Program of China, Stem Cell and Translational Research (no. 2016YFA0100300), the National Natural Science Foundation of China (no. 31861143016 and no. 31971346; NSFC. no. 31470834, no. 31522017, and no. 31670869), the Science and Technology Commission of Shanghai Municipality (no. 18JC1411000 and no. 14JC1401700), the Thousand Youth Talents Plan of China to H.Y., and the Fundamental Research Funds for the Central Universities. This work was also partially supported by the National Key R&D Program of China (no. 2017YFC1103704) and the Sanming Project of Medicine in Shenzhen (no. SZSM201412020) to L.M. **Author contributions:** H.Y. conceived this study. H.Y. and J.Y. designed the project. J.Y., L.Y., L.M., J.J., S.X., K.D., X.W., Y.X., and Y.L. performed the experimental work. L.M. and Y.L. performed the monkey experiments. H.Y., J.Y., L.Y., and L.M. analyzed the results and wrote the manuscript. All authors edited and approved the manuscript. **Competing interests:** H.Y., J.Y., and L.Y. are inventors on patent applications (Chinese patent application nos. 201710797238.5 and 201710796698.6) submitted by ECNU that cover the methods and applications of PCA-controlled transgene expression switches. All other authors declare that they have no competing interests. **Data and materials availability:** All data associated with this study are present in the paper or the Supplementary Materials. All genetic components related to this paper are available with a material transfer agreement and can be requested from H.Y. (hfye@bio.ecnu.edu.cn).

Submitted 29 October 2018

Resubmitted 20 May 2019

Accepted 27 August 2019

Published 23 October 2019

10.1126/scitranslmed.aav8826

Citation: J. Yin, L. Yang, L. Mou, K. Dong, J. Jiang, S. Xue, Y. Xu, X. Wang, Y. Lu, H. Ye, A green tea-triggered genetic control system for treating diabetes in mice and monkeys. *Sci. Transl. Med.* **11**, eaav8826 (2019).

Science Translational Medicine

A green tea–triggered genetic control system for treating diabetes in mice and monkeys

Jianli Yin, Linfeng Yang, Lisha Mou, Kaili Dong, Jian Jiang, Shuai Xue, Ying Xu, Xinyi Wang, Ying Lu and Haifeng Ye

Sci Transl Med 11, eaav8826.
DOI: 10.1126/scitranslmed.aav8826

Tea for type 1 and type 2 diabetes

Cell therapy is a promising approach for diabetes. Yin *et al.* developed an elegant control system by engineering cells to respond to protocatechuic acid, a metabolite in green tea. Orally ingested protocatechuic acid regulated blood glucose by triggering secretion of insulin or a short variant of human glucagon-like peptide 1 from implanted engineered cells in mouse and nonhuman primate models of type 1 and type 2 diabetes. This study demonstrates the versatility of synthetic biology for developing remotely controlled cell-based therapies for diabetes.

ARTICLE TOOLS

<http://stm.science.org/content/11/515/eaav8826>

SUPPLEMENTARY MATERIALS

<http://stm.science.org/content/suppl/2019/10/21/11.515.eaav8826.DC1>

RELATED CONTENT

<http://stm.science.org/content/scitransmed/9/387/eaal2298.full>
<http://stm.science.org/content/scitransmed/7/318/318ra201.full>
<http://stm.science.org/content/scitransmed/10/437/eaap8562.full>
<http://stm.science.org/content/scitransmed/7/289/289ra84.full>
<http://stm.science.org/content/scitransmed/3/106/106ps42.full>

REFERENCES

This article cites 63 articles, 13 of which you can access for free
<http://stm.science.org/content/11/515/eaav8826#BIBL>

PERMISSIONS

<http://www.science.org/help/reprints-and-permissions>

Use of this article is subject to the [Terms of Service](#)

Science Translational Medicine (ISSN 1946-6242) is published by the American Association for the Advancement of Science, 1200 New York Avenue NW, Washington, DC 20005. 2017 © The Authors, some rights reserved; exclusive licensee American Association for the Advancement of Science. No claim to original U.S. Government Works. The title *Science Translational Medicine* is a registered trademark of AAAS.